



Deliverable D3.9b Verification of the fibre optic sunlight illumination system

Version: V0.1

Project details:	
No:	211948
Name:	clear-up
Title:	Clean buildings along with resource efficiency enhancement using appropriate materials and technology
Start date:	01/11/2008
Duration:	48 month

Dissemination Level		
PU	Public	
PP	Restricted to other programme participants (including the Commission Services)	
RE	Restricted to a group specified by the consortium (including the Commission Services)	
CO	Confidential, only for members of the consortium (including the Commission Services)	X

Document details:	
Project	clear-up
Title	Deliverable D3.9b Verification of the fibre optic sunlight illumination system
Version	0.1
Workpackage	WP1
Author(s)	Tarja Volotinen and David Lingfors, Uppsala University
Keywords	Solar lighting system, illumination performance, energy saving, light balancing
Document ID	clear-up-- shortname-V0.1-DD/MM/YYYY
Synopsis	<p>The fiber optic solar lighting system:</p> <ul style="list-style-type: none"> Parans SP3, has been tested at Uppsala University for the illumination performance, energy saving and light balancing with fluorescent electric lights. The system luminaires have been installed in a test site of a study hall and corridor area.¹⁻² The significant results are: The illumination at the test site using solar light was at least as high as when using the artificial lights and even higher at very clear days. The luminous flux output was 500 lm per luminaire at 100 000 lx direct sun illuminance and at 130 000 lx it was 770 lm per luminaire for a 10 m fiber distance. The sunlight output coupling efficiency was 23 %. However, for a 20 m SP3 system the luminous flux output (400 lm) at 100 000 lx was higher than specified (350 lm). The SP3 system of Parans provides high quality solar light of a full spectrum, close to the spectrum of the sun. The spectrum of fluorescent lights of the test site consists of a few narrow peaks. The correlated color temperature of the light from the SP3 system was 5800±300 K and the color rendering index 85 at the 10 m fiber distance. The corresponding values for the fluorescent lights of the test site are 3180 K and 77 respectively. The lighting energy saved due to decreased need for artificial light was estimated to 19 % in Uppsala which has 1790 annually sun hours. The savings in Italy, which has 3400 sun hours, is 46 %. Additional saving, especially in warmer countries can be obtained due to decreased need for cooling in the building as the solar luminaires provide negligible heat to the surrounding air. Economical saving could also be realized by improved well-being of the occupants spending time under the solar luminaires. Clear indication of the heating caused by the electric lights, and the cooling of the air, when the solar lights were on, was obtained. The verification of the cooling energy saving is under investigation. Three ways of balancing the artificial light due to sunshine fluctuations have been investigated. The global horizontal irradiance could not be used as a control signal for balancing the artificial lights, because it is not related to the light coupled into the sun-tracking system. A signal from a pyranometer attached to the SP3 sun tracking collector was usable. Also the signal from an indoor luxmeter sensor could be used for balancing the light. However the signal from the light sensor which makes the SP3 collector to track the sun is probably the most cost effective method as it would serve two purposes; tracking the sun and balancing the artificial lights. Effective light diffusers have been developed (Task 3.5b) and tested. The results show that the new diffusers increase the light distribution angle by a factor two and the illuminated area by a factor four. A patent application is under preparation³
Release Date	22/11/2012

Revision history:			
Version	Date	Changes	changes by
0.1	22/11/2012	First development	Tarja Volotinen (UU)

Verification of the fibre optic sunlight illumination system

PREFACE

This study has been mainly performed as a master thesis in the program Energy Systems Engineering at Uppsala University (UU). The work was carried out by David Lingfors at the Div. of Solid State Physics, Dept. of Engineering Sciences, the Ångström Laboratory, from January to October 2012 at half time. Supervisor was Doc. Tarja Volotinen (Div. of Solid State Physics, UU), Reviewer Prof. Arne Roos (Div. of Solid State Physics, UU) and Examiner Lect. Kjell Pernestål (Dept. of Physics and Astronomy, UU).

The entire costs for the personnel, laboratory equipment and other project costs at the Div. of Solid State Physics for this study, not specified in David's Acknowledgement of his thesis, were paid from the grant of the Clear-up Project, which is warmly acknowledged.

This document is created by attaching the MSc thesis of David Lingfors into the this start document.

DIV. OF SOLID STATE PHYSICS, DEPT. OF ENGINEERING SCIENCES, UPPSALA UNIVERSITY

Illumination properties and energy savings of a solar fiber optic lighting system balanced by artificial lights
MSc study for the engineering program in Energy Systems

David Lingfors

2012-11-15

Abstract

A solar fiber optic lighting system, SP3 from the Swedish company Parans Solar Lighting AB, has been installed in a study area/corridor test site. A collector is tracking the sun during daytime, focusing the direct sun irradiance via Fresnel lenses into optical fibers, which guide the solar light into the building. The illumination properties of the system have been characterized. The energy saving due to reduced need of artificial lighting have been calculated and methods for balancing the artificial lights in the test site have been evaluated.

The illumination at the test site using solar light was at least as high as when using the artificial lights and even higher at very clear days. The luminous flux output (500 lm) was somewhat lower than specified by the manufacturer (550 lm) at 100 000 direct sun illuminance. The output at 130 000 klx was high 767 ± 33 lm the sunlight coupling efficiency 23 %. However, for a 20 m SP3 system the luminous flux output (400 lm) at 100 000 lx was higher than specified (350 lm).

The SP3 system of Parans provides high quality solar light. It has a fuller spectrum close to the spectrum of the sun compared to the fluorescent lights at the test site. The correlated color temperature of the system was 5800 ± 300 K and the color rendering index 84.9 ± 0.5 .

The lighting energy saved due to decreased need for artificial light was estimated to 19 % in Uppsala which has 1790 annually sun hours. The savings in Italy, which has 3400 sun hours, is 46 %. Additional saving, especially in warmer countries can be obtained due to decreased need for cooling in the building as the solar luminaires provide negligible heat to the surrounding air. Economical saving could also be realized by improved well-being of the occupants spending time under the solar luminaires.

Three ways of balancing the artificial light due to sunshine fluctuations have been investigated. The global horizontal irradiance could not be used as a control signal for balancing the artificial lights but a pyranometer attached to the SP3 sun tracking collector was usable. Also the signal from an indoor luxmeter sensor could be used for balancing the light. However the signal from the light sensor which makes the SP3 collector to track the sun is probably the most cost effective method as it would serve two purposes; tracking the sun and balancing the artificial lights.

Executive summary

In this study a solar fiber optic lighting system is characterized. The system gives full spectrum light similar to the sun which has a positive impact on the well being of human beings. The system illuminates a study hall / corridor area of about 45 m² on sunny days at least as good as regular fluorescent lights do. The annual lighting energy savings are 19 % in Uppsala, but in sunnier countries up to 46 %. Savings due to decreased need for cooling in sunny countries are yet to be investigated but could be significant.

Populärvetenskaplig sammanfattning

Ett solbelysningsystem har testats på Ångströmlaboratoriet i Uppsala. En panel bestående av 36 linser är placerat på taket och följer solen under dagen med hjälp av en sensor som känner av solens riktning. Varje lins fokuserar solljuset till varsin optisk fiber och solljuset leds sedan in i byggnaden till lokaler som har väldigt dålig eller ingen tillgång till dagsljus från fönster. Studien visar även att relativt mycket ljus kan kopplas genom systemet. För ett system med 10 meter fiber kommer 23 % av den synliga delen av solljuset som träffar solpanelen genom fibrerna. Denna studie visar att kvalitén på solljuset som leds in genom fibern är mycket hög. Spektrumet liknar i stor utsträckning det spektrum som solen har.

Systemet drar väldigt lite energi, och har för Uppsala uppskattats ge en besparing av elbelysning på 19 %. Energibesparingen skulle bli större i ett land som har fler soltimmar än Uppsala; i exempelvis Italien 46 %. Det tar dock lång tid att få igen investeringen av systemet. Istället måste hänsyn tas till de positiva effekter som solljus har på vårt välbefinnande. Studier visar att vår dygnsrytm påverkas av vilket ljus vi vistas i eftersom den icke visuella ljusreceptorn melanosin slutar producera hormonet melatonin när den utsätts för blått ljus kring 460 nm, av vilket den optiska effekten är hög i solljus relativt många artificiella ljuskällor. De positiva hälsoeffekterna kan ge finansiella besparingar på längre sikt.

I studien har också olika sätt att balansera ljusnivån genom att dimma elbelysningen studerats. Två sätt har visat sig fungera; dels genom att styra ljusnivån med hjälp av ljussensor inne i testmiljön och dels genom att montera en pyranometer på den solföljande panelen. Det bästa sättet vore förmodligen att använda den ljussensor som är installerat på panelen för att följa solen. På så sätt behöver ingen extra sensor köpas till, och ljusstyrningen blir kostnadseffektiv.

Acknowledgements

First I would like to give my warmest thanks to my supervisor Doc. Tarja Volotinen and Prof. Claes-Göran Granqvist for giving me the opportunity and support to study this interesting subject at the div. of Solid State Physics at the Ångström Laboratory, Uppsala University. I would also like to give my sincere thanks to Akademiska hus, Mats Wieselblad for financing the sensors, dimming of the lights, the weblogging system and the installation of the SP3 system. A sincere thank you also to Energy House Project, Dr. Carla Puglia who bought the SP3 system and Ångström Material Academy (ÅMA) for the financing of some parts of the measurement equipment. I would also like to thank Parans Solar Lighting AB and especially Rebecca Hallqvist and Daniel Johansson for their collaboration. For the support in my daily work I want to thank Andreas Mattson and Bengt Götesson for solving some practical problems, and also from my reviewer Prof. Arne Roos. I want to thank Bravida for the support of the installation of the system and especially Mikael Magnusson, who always answered my questions about the jumble of electrical circuits around the test site. I would also like to show my gratitude to Mikael Österberg for the creation of the database function, enabling the data from the test site. Thanks also to Uwe Zimmerman for providing solar irradiation data.

Finally I would like to thank my girlfriend Lovisa for her great support. She gave me love and energy to pull through the tough periods of this work.

Preface

This work was performed as a master thesis in the program Energy Systems Engineering at Uppsala University (UU). The work was carried out at the Div. of Solid State Physics, Dept. of Engineering Sciences, the Ångström Laboratory, from January to October 2012 at half time. Supervisor was Doc. Tarja Volotinen (Div. of Solid State Physics, UU), Reviewer Prof. Arne Roos (Div. of Solid State Physics, UU) and Examiner Lect. Kjell Pernestål (Dept. of Physics and Astronomy, UU).

Contents

1	Introduction.....	7
1.1	Background.....	7
1.2	Problem description and motivation.....	8
1.3	Aim.....	9
2	Theory of light.....	9
2.1	Definition of photometric quantities.....	9
2.2	Color of light.....	12
3	Solar fiber optic lighting systems.....	15
3.1	Components characteristics and their losses.....	16
3.2	SP3 solar light system.....	18
3.3	Himawari solar lighting system.....	19
3.4	TR5-1 solar light system.....	19
4	Methods.....	19
4.1	Experimental methods.....	19
4.2	The setup of the test site.....	24
5	Results.....	31
5.1	System components.....	31
5.2	The solar lighting system.....	33
5.3	Balancing of the artificial light.....	39
5.4	Energy saving.....	41
6	Discussion.....	44
6.1	Sources of error.....	44
6.2	Health benefits - Circadian rhythm affected by the spectrum of light.....	44
6.3	Lessons learned along the way.....	45
6.4	Future challenges.....	45
7	Conclusions.....	46
	References.....	47
	Appendix A – Questionnaire for the evaluation of the lighting environment.....	50

Abbreviations

CCT	Correlated Color Temperature
CIE	Commission Internationale de l'Éclairage (eng. International commission on illumination)
CQS	Color Quality Standard
CRI	Color Rendering Index
CRM	Color Rendering Map
LER	Luminous Efficacy of Radiation
NIR	Near InfraRed
OMIS	Own Manufactured Integrating Sphere
PMMA	<u>P</u> o <u>l</u> y <u>m</u> e <u>t</u> h <u>y</u> l <u>m</u> e <u>t</u> h <u>a</u> c <u>r</u> y <u>l</u> a <u>t</u> e
POF	Plastic optical fiber
SPD	Spectral Power Distribution
VIS	Visual Spectrum of light

1 Introduction

1.1 Background

Today we spend more time inside than we did hundred years ago. Working eight hours a day at large office complexes everyone is not fortunate to sit close to a window having natural light flooding their desks. Instead people spend their working day under artificial light.

A new technology is offering a solution; a fiber optic solar lighting system. The sunlight is collected and focused by a sun tracking array of lenses on the roof or façade of a building and then guided into the building through optical fibers to rooms with insufficient or no natural light. On sunny days solar light is used for illumination and when cloudy or dark, artificial lights are still needed. In this way energy can be saved and the well being of the occupants is increased without need for large reconstructions.

There are many arguments for choosing natural light. Previous studies show that the human body is best adapted to natural light^{1,2,3}. Light is not only essential for performing visual tasks but also affect biological functions in the body. For instance, the rate of secretion of the hormone Melatonin in the pineal gland depends on the light conditions⁴. Melatonin regulates the circadian rhythm or sleep/wake cycle, and also the immune system, aging, reproduction system and respiration for instance^{5,6}.

Natural light and full-spectrum artificial light are shown to more efficiently restrain the melatonin secretion during daytime, which implies that we feel more alert and awake when exposed to full-spectrum light⁷. Studies have shown positive effects on exposure of natural light instead of artificial on indoor occupants during daytime, such as less headaches and eyestrains, less absenteeism at work or school, higher productivity/grades and higher sale pressure in retails^{1,2,8,9,10}.

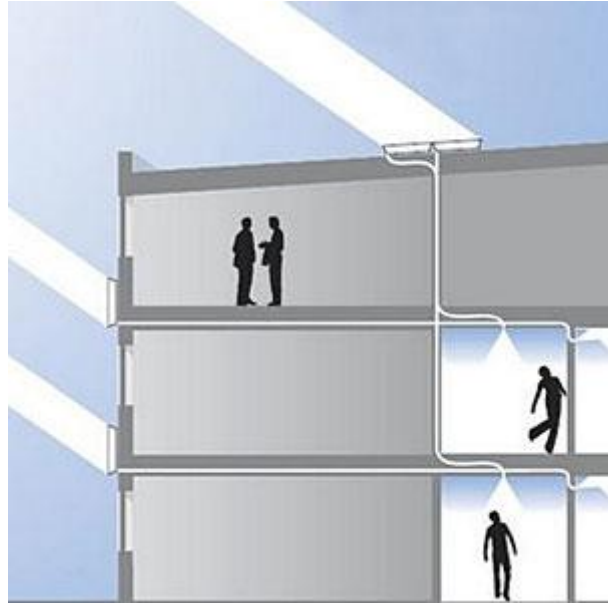


Figure 1. The principal function of a solar fibre optic lighting system. The sunlight is collected and guided into darker interiors of the building (www.parans.com).

Beyond the above mentioned benefits of natural light, designing of buildings for efficient utilization of daylight leads to a decreasing need of artificial light and therefore saving of energy. One example is the Lockheed Martin office complex in San Francisco, which was designed to better utilize the daylight by skylights and an atrium in the center of the building, which were estimated to result in a reduction of 50 % in energy costs or \$0.5 million/year. The savings were due to less artificial light and less cooling because of reduced heat gain from artificial light. The extra investment cost of \$2 million for the energy efficient building is paid back in four years, not taking productivity increase into account, which the company estimated to \$2 million yearly because of the improved work environment^{8,11}.

1.2 Problem description and motivation

The Lockheed Martin example illustrates the benefits of daylight systems in large commercial buildings. However, it is expensive to build new or refurbish existing buildings with skylights and atriums. The energy savings seen in San Francisco might not be that significant in northern Europe where cold winters mean high energy leakage through windows and skylights.

In this study the SP3 system provided by Parans Solar Lighting AB, Sweden (Parans) was studied. Their system focuses the sunlight by lenses on the roof or façade and guides the light by optical fibers into the building. Guiding light through optical fibers is not a new idea, and can be found in literature as early as 1958¹², but has not been seriously considered until the past decades with arousing concern of energy efficiency in buildings.

This study focuses on the characterization of the Parans SP3 system; how much light the system can deliver during various weather conditions and seasons, and what potential energy saving this corresponds to. The color properties of the solar light through the system is also characterized to conclude whether it can be considered as healthy and of comparable quality as natural

light outside or through windows and skylights. The optimal regulation technique for balancing solar light and artificial light are not fully known and different approaches were investigated.

1.3 Aim

The main questions that are strived to be answered are:

1. What are the illumination properties of the SP3 system in terms of illuminance, spatial distribution, luminous flux output and color properties?
2. Are there any positive effects on the human well being when exposed to the solar light of the SP3 system?
3. How much energy can be saved in terms of electrical power and decreased need for cooling?
4. How can the balancing of the artificial light versus the solar light be controlled most accurately?

2 Theory of light

Visible light in its most fundamental definition is electromagnetic waves with wavelengths that range from 380 nm to 780 nm. The basic source of light on earth is the sun, which also emits electromagnetic waves in the ultra violet (UV), near infrared (NIR) and long IR wavelength (heat) part of the electromagnetic spectrum.

2.1 Definition of photometric quantities

Light is in physics characterized in radiometric quantities. When dealing with the visual aspects of light, radiometric values must be transformed with respect to the sensitivity of the human eye from radiometric to photometric units (Figure 3). The following photometric quantities were used in this work to characterize the lighting properties of the SP3 system.

2.1.1 Energy of light

In radiometric terms the power of light is measured as **optical power** (Watt, W), but taking the sensitivity of the eye into account, the energy can be expressed in the photometric quantity **luminous flux** (lumen, lm). The relationship between radiometric and photometric quantities is defined as;

“A monochromatic light source emitting an optical power of 1/683 watt (= 1.46 mW) at 555 nm has a luminous flux of 1 lumen (lm)”¹⁵

2.1.2 Spectral power distribution

The power emitted for each wavelength by a light source can be represented in a graph as the **spectral power distribution** (SPD)¹³. Generally the **power** could be any quantity representing the light intensity, such as radiant power or optical power. Which quantity should be defined whenever the SPD concept is used¹⁴. In Figure 2 the SPD is represented as the radiant power in watts per square centimeter incident on the atmosphere (yellow) and earth (orange) respectively as a function of wavelength.

When considering the color of light the color adaption of the human eye needs to be taken into account. The human eye is most sensitive to wavelengths around 555 nm (Figure 3)¹⁵. In those cases the intensity relative photometric quantities is appropriate when illustrating the SPD.

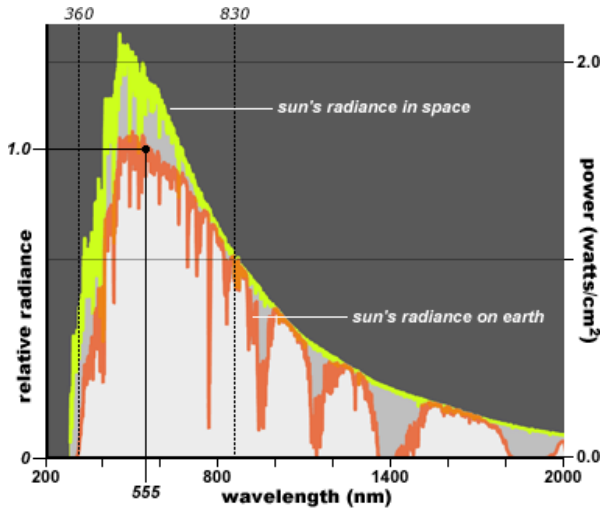


Figure 2. Spectral power distribution (SPD) of the sun radiance in space (yellow) and on earth (orange). The difference between the curves is due to efficient absorption of certain wavelengths in the atmosphere, for instance in ozone and water vapor.¹³

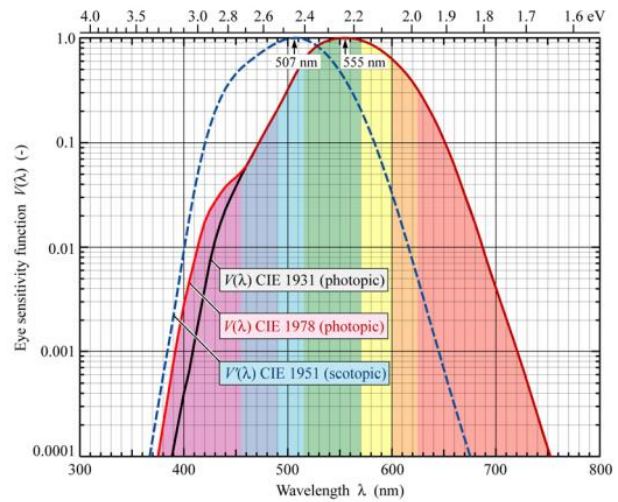


Figure 3. The relative sensitivity of the human eye to color of light for the CIE 1931 photopic vision and the later modified CIE 1978 photopic vision and also the CIE 1951 scotopic vision used in colorimetry at ambient light¹⁵.

2.1.3 Luminous intensity

The luminous flux radiated in the solid angle of 1 steradian (Figure 4) is called **luminous intensity** and has the unit candela (cd), hence 1 cd is equal to 1 lm/sr¹⁶. The luminous intensity varies for different positions under a light source. These variations can be illustrated in a **polar diagram** (Figure 6), which describes the **luminous intensity distribution** of a light source. If the light distribution is uniform around the vertical axis, only one curve needs to fully represent the light distribution of a light source. In the case of non-uniformity two or three curves are meaningful. Figure 5 shows six half planes, the basic four are C0, C90, C180 and C270 or the C0-180 and C90-270 whole planes. The C90-270 plane is always perpendicular to the C0-180 plane. Normally the C0 plane is chosen where the maximum luminous intensity is measured, but in cases where the light source is situated relative an object, the C0-180 plane is chosen perpendicular to the extension of the object, for instance a corridor or a road. In Figure 5 the C45-225 plane represents where the maximum luminous intensity has been measured, and the C0-180 plane is perpendicular to the axis of the light source. The same C45-225 plane is illustrated as the red curve in Figure 6. The luminous intensity in the polar diagram is denoted as candela per 1000 lumen.

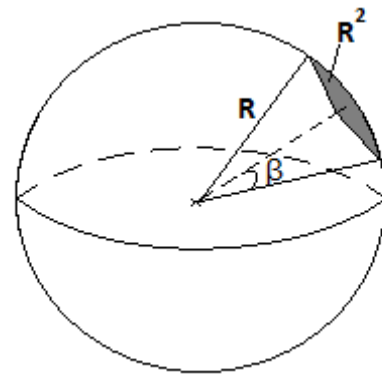


Figure 4. The solid angle β of the half cone is defined as 1 steradian (sr) when the surface of the spherical cap (grey) is equal to the square of the radius R of the sphere. $1 \text{ sr} = 32.77^\circ$.

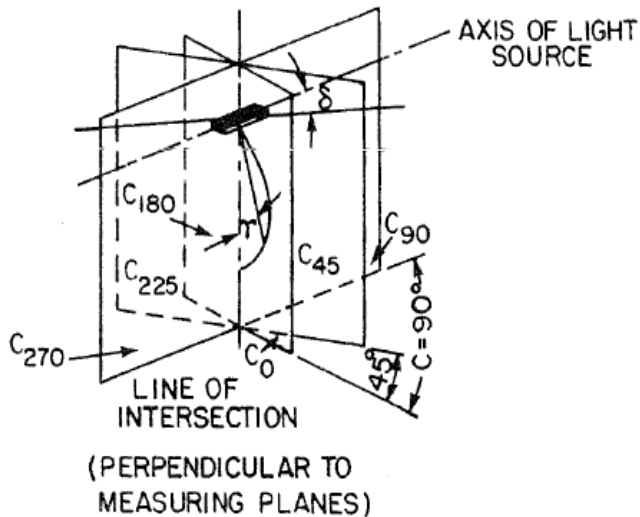


Figure 5. C-planes for measuring the luminous intensity distribution of a luminaire¹⁶.

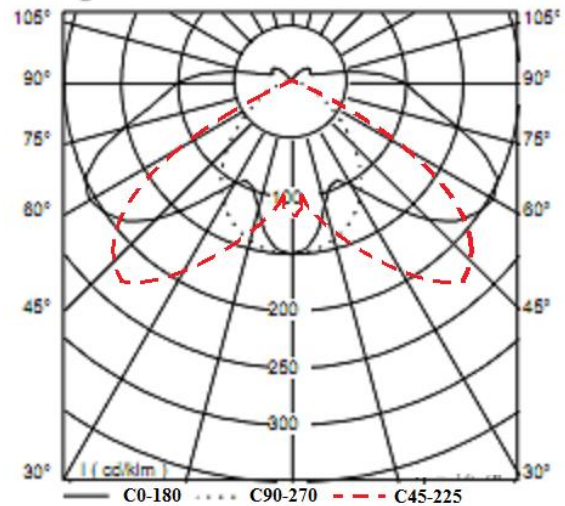


Figure 6. Polar diagram showing the luminous intensity distribution of a luminaire, in three planes. (Modified from electronic resource; http://www.lumiance-lighting.com/pdf/LIGHT_GD.pdf, red part added).

2.1.4 Luminous efficacy of radiation

To describe how efficiently electrical power is transformed into light in an artificial luminaire in terms of luminous flux, the **luminous efficacy of radiation (LER)** can be calculated as the ratio between the input electric power and the output luminous flux (W/lm). The electrical power should not be confused with the optical power. For the SP3 system the corresponding LER is calculated as the ratio between the consumed electric power of the collector motors and the luminous flux of the solar luminaire.

2.1.5 Illuminance

Illuminance is the luminous flux per area unit (lm/m² or lx)¹⁶. An EU standard (EN 12464-1:2002), defines the minimum illuminance at 85 cm from the floor for different kinds of indoor locations¹⁷.

2.2 Color of light

In addition to the luminous flux, LER and illuminance there are other important characteristics of light. For instance, the color properties influence how we perceive the world around us. Besides the visual performance, the color of light can also have great impact on the biological systems in the body. This issue is discussed in the introduction. Other aspects like flickering and glaring that affect the visual performance were not technically measured but were subjectively evaluated through an inquiry (Chapter 4.2.8 and 5.2.6).

Depending on light source, the objects illuminated appear to render different colors. A good color rendering can be crucial in some professions. The color of light from a specific light source can roughly be defined by the correlated color temperature (CCT)¹⁸. Given that two light sources have the same CCT, the color rendering can vary; the Color Rendering Index (CRI) of a light source describes how well eight color samples are rendered by the light source relative a standard illuminant with equal CCT defined by CIE. The method for calculating the CRI was first published in 1965 and has been revised since then, latest version published in 1995¹⁹. For some applications it is considered outdated and modifications of the method have been suggested²⁰ and in some cases new methods for determining the quality of light, like the Color Quality Scale (CQS), the CIECAM02 and the Color Rendering Map (CRM) have been proposed^{21,22,23}. The CRM method was developed to work as a visually intuitive tool for determination of the color rendering which a single value like CCT or CRI cannot provide. As Figure 7 shows, light sources of identical CCT and CRI can have very different spectra, which imply that the CRM is motivated.

The attempts of finding a new method of determining the color properties of light are in many cases due to the development of new light sources (LED, fluorescent etc.). In this work CCT, CRI and SPD illustrations have been considered sufficient for evaluating and comparing different light sources; first because they're well established standards and secondly because the initial purpose of CRI was to compare tungsten lamps, which are black body radiators like the sun.

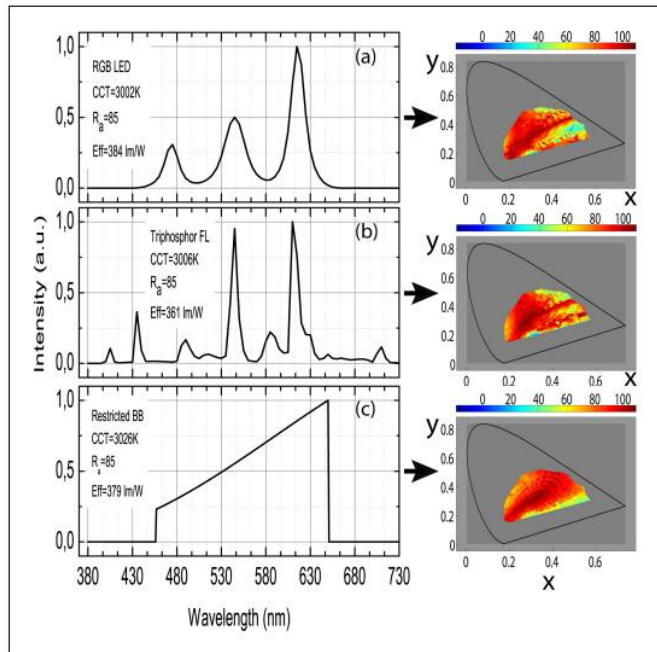


Figure 7. To the left the SPD, CCT, CRI and LER of three different light sources; RGB LED (a), Triphosphor fluorescent lamp (b) and a band pass filtered black body radiator (c). To the right are the corresponding CRM for the light sources²³.

From the SPD of a light source chromaticity coordinates (x,y,z) can be derived, using methods developed by CIE. Two different methods of calculating the CIE chromaticity coordinates have been developed during the 20th century; CIE 1931 2° standard observer and the CIE 1964 10° standard observer. *Color matching functions* $(\bar{x}, \bar{y}, \bar{z})$ in the range of 380 nm to 780 nm and a step of 1 nm has been derived in correlation with the sensitivity of the human eye (Figure 8) by CIE for the two standards. The 2° observer is the most commonly used and therefore implemented in this study.

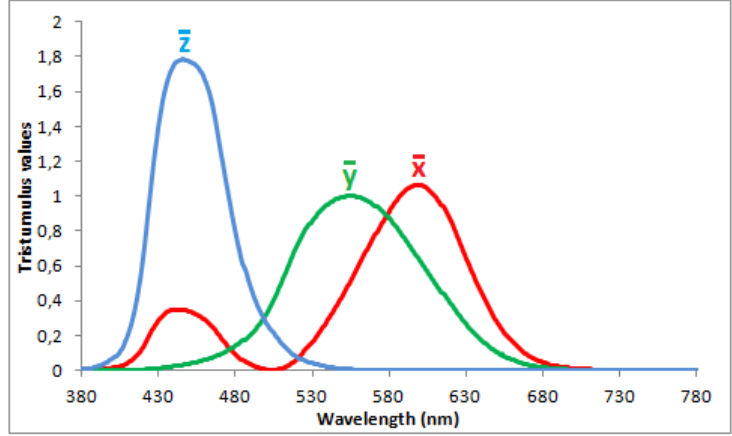


Figure 8. The color matching functions of the CIE 1931 2° standard observer.

The chromaticity coordinates are calculated as follows;

$$x = \frac{X}{X + Y + Z} \quad (1)$$

$$y = \frac{Y}{X + Y + Z} \quad (2)$$

$$z = \frac{Z}{X + Y + Z} \quad (3)$$

where X, Y and Z are the Tristimulus values and are calculated as;

$$X = \sum_{380}^{780} [E(\lambda)\bar{x}(\lambda)\Delta(\lambda)] \quad (4)$$

$$Y = \sum_{380}^{780} [E(\lambda)\bar{y}(\lambda)\Delta(\lambda)] \quad (5)$$

$$Z = \sum_{380}^{780} [E(\lambda)\bar{z}(\lambda)\Delta(\lambda)] \quad (6)$$

where $E(\lambda)$ is the relative radiometric intensity as a function of the wavelength, $\bar{x}(\lambda)$, $\bar{y}(\lambda)$, $\bar{z}(\lambda)$ are the CIE 1931 color matching functions and $\Delta(\lambda)$ is the wavelength interval.

The calculated chromaticity coordinates (x,y) can be pinpointed at the CIE 1931 Chromaticity Diagram (Figure 9). From the chromaticity coordinates the CCT can easily be obtained by the polynomial formula developed by McCamy¹⁸;

$$CCT = -449n^3 + 3525n^2 - 6523.3n + 5520.33, \quad (7)$$

where $n=(x-x_e)/(y-y_e)$ and $(x_e=0.3320, y_e=0.1858)$ are the epicenter of the black body curve seen in Figure 9.

The McCamy polynomial function is an approximation of the black curve seen in Figure 9. The computation of the CRI is a complex procedure referred to as the **Test Sample Method** (explained in CIE 13.3-1995¹⁹) and was calculated through a supplied software of the CIE 13.3-1995 (*Disk D008, rel. 2.0*).

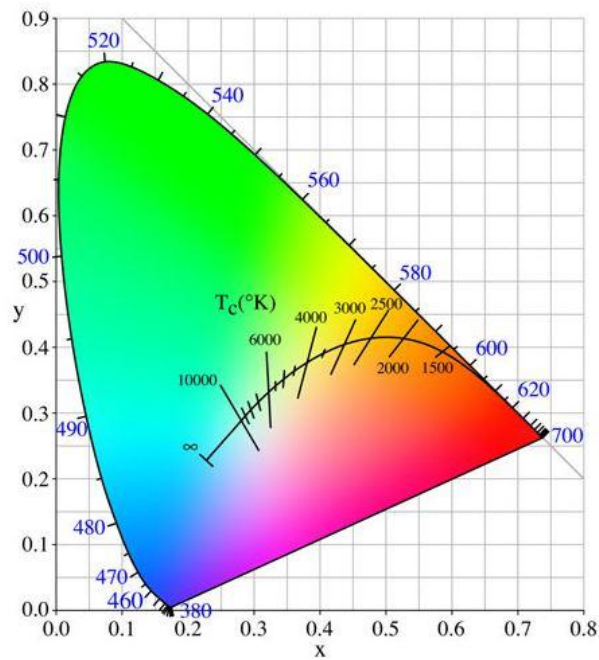


Figure 9. The CIE 1931 Chromaticity Diagram. The point on the black curve closest to the x,y-coordinate of the test sample can be observed as the CCT (Retrieved from <http://www.ledropelightsandmore.com/color-temperature.html>, 2012-09-14).

3 Solar fiber optic lighting systems

The SP3 system evaluated in this work is a solar fiber optic lighting system. The basic principle of such a system is described in Figure 10. A collector consisting of a matrix of lenses tracks the sun. The direct component of the solar light is focused by each lens into an optical fiber, via a filter, which reflects the ultraviolet (UV), and near infrared (NIR) parts of the solar light. The diffuse component is not coupled into the fibers. The light is guided through the fibers into the rooms that need to be lit. The guiding is possible due to total internal reflection which occurs at the interface of the core and cladding²⁴. The refractive index of the core (n_0) and cladding (n_1) are different, normally $n_0 > n_1$ (

Figure 11)²⁵. An optical fiber is often characterized by its numerical aperture (NA), which is determined by the relation between the refraction index of the core and cladding as;

$$NA = \sin \theta = \sqrt{n_0^2 - n_1^2}, \quad (8)$$

where θ is the half acceptance angle, n_0 and n_1 are the refractive indexes of the core and cladding, respectively (Figure 11).

If the incident angle is greater than the acceptance angle θ the light is not guided, but continues through the cladding and leaks out of the fiber. The incident angle of the light is also the output angle of the light, but the light intensity is normally higher nearer the axis of the fiber as can be seen in Figure 12.

Like in most solar fiber optic lighting systems, the fibers are assembled into bundles to get the appropriate luminous flux output from the solar luminaires of the SP3 system.

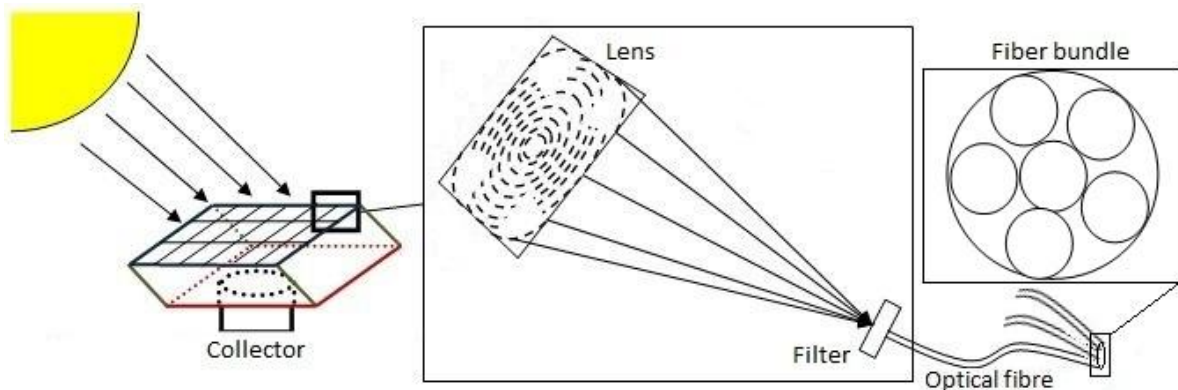


Figure 10. A schematic of a solar fiber optic lighting system.

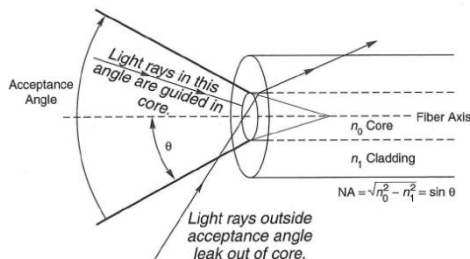


Figure 11. The principle of light guidance in optical fibers.

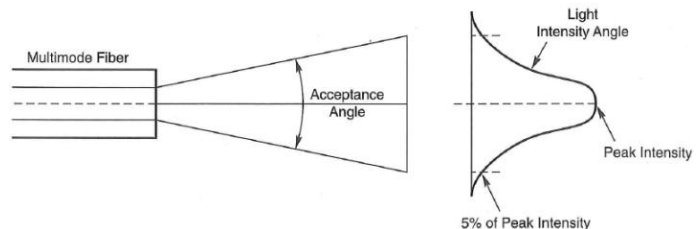


Figure 12. The output angle is equal to the acceptance angle (left). To the right the typical angle dependent intensity distribution is illustrated²⁵.

3.1 Components characteristics and their losses

3.1.1 The Fresnel lens

A Fresnel lens is built up by using only the refractive parts of an ordinary lens put side by side as Figure 13 shows. The main advantage of such a lens is the low manufacture costs but also in application where space is a limiting factor as in OH projectors and copy machines. Fresnel lenses are used in the SP3 system and are constructed by imprinting a pattern of silicone onto a glass plate.

The direct solar light is actually not parallel beams because the extent of the sun. Therefore it is impossible to have a perfect focal spot without using at least two lenses. There are other lens faults that prevent the focal spot to be sufficiently small. The incident rays refracted near the edges for some lenses cross the center axis in another point than rays refracted closer to the center axis. This is called **spherical aberration** (Figure 14a). This aberration could be limited by polishing the edges. The refractive index is wavelength dependent, which results in dispersion of the light. This phenomenon is called **chromatic aberration** (Figure 14b). The spherical and chromatic aberrations of single lenses are normally reduced by using an achromatic doublet, which consists of a biconvex lens, joined with a concave lens (Figure 14c). As the name suggests, the achromatic doublet was initially only reducing the chromatic aberration but are today normally also designed to reduce the spherical aberration. The focal spot can be minimized by varying the material composition of the lenses of the doublet, add an airgap between the lenses or even using multiple merged lenses²⁶. An appropriate design can efficiently limit the dispersion, but increased complexity also means increased cost. The achromatic doublet is a conventional technique and is used in many common applications such as cameras and telescopes.

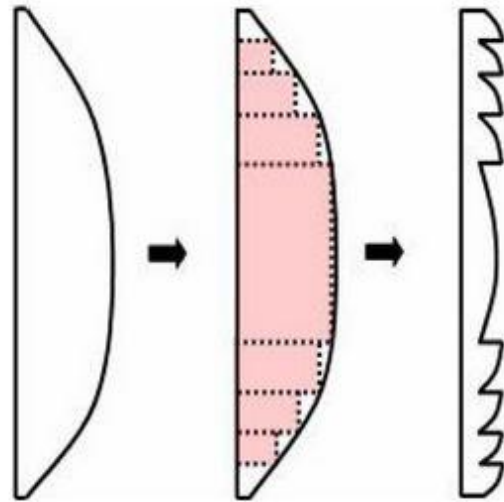


Figure 13. In the Fresnel lens materials that don't contribute to the optical characteristics of the lens is removed (Retrieved from <http://spie.org/x8645.xml> 2012-09-12).

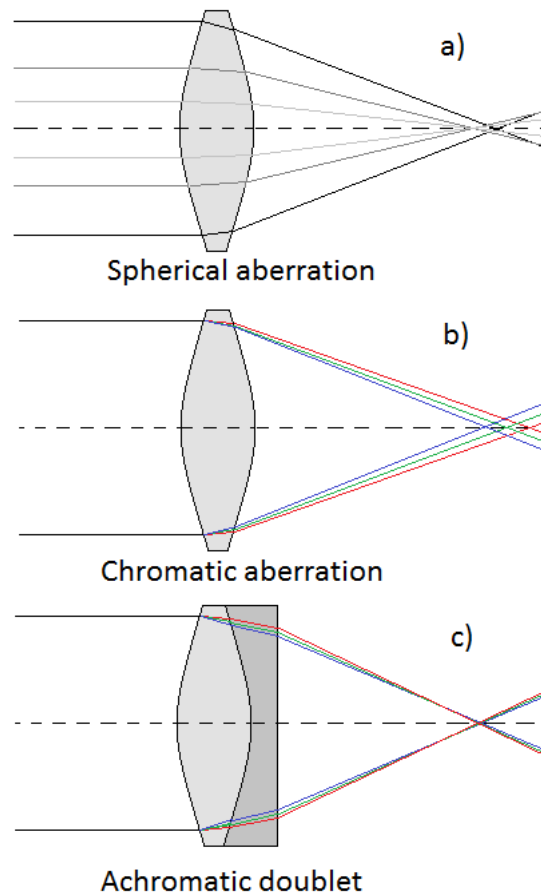


Figure 14. Common defects in single lenses; spherical and chromatic aberrations can be limited by using an achromatic doublet.

3.1.2 The filter

There are mainly two kinds of filters used for limiting transmitted light to certain wavelengths; reflecting and absorbing filters. The latter is not desirable for the SP3 system as absorption accumulates heat, which can damage the fiber or the glue between the fiber and connector. High reflection and low absorption is especially important if the fiber is made of plastic, which normally has lower heat resistance than glass. The filter of the SP3 system is of the reflective type and reflects UV and NIR but transmits visual light (VIS). The transmittance of VIS is high with low losses, due to an antireflective coating for VIS.

3.1.3 The Plastic Optical Fiber (POF)

The losses in a plastic optical fiber (POF) are greater than in glass fibers. The typical losses in glass fibers are not described in this work. Both UV and NIR light can damage the POF. It has been shown that the main losses in POF are due to vibrational absorption in the CH-bindings of the PMMA molecule (Figure 15) when exposed to infrared radiation.

Figure 16 shows the typical spectral attenuation of a PMMA POF. The attenuation peaks occur periodically and the three main attenuation peaks in the visual spectrum around 545, 625 nm and 730 nm are overtones of peaks of greater magnitude in the infrared spectrum. If replacing the hydrogen atoms with deuterium the total loss could be reduced.²⁶

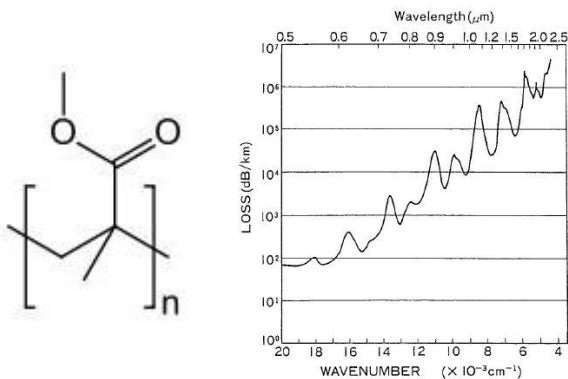


Figure 15. The PMMA molecule. Figure 16. Typical spectral attenuation of a PMMA POF²⁷.

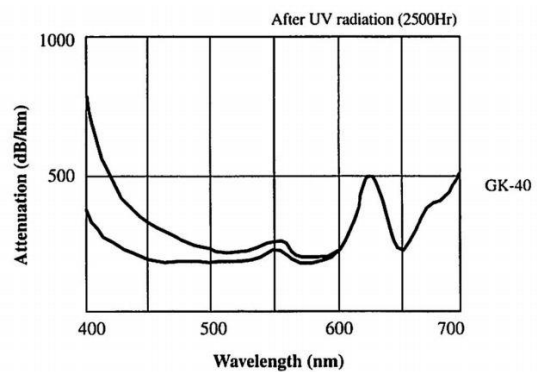


Figure 17. The attenuation has increased for a PMMA POF after 2500 hours exposure of UV light²⁸. The light intensity is not given.

Figure 17 shows the expected increase in attenuation (dB/km) after the POF was exposed to UV radiation for 2500 hours²⁸. This proves the importance of a filter with high performance and durability. Otherwise the POF and the solar light system will degrade over time.

Mode attenuation needs also to be considered for thick multimode fibers. Light that is coupled into the fiber in an angle will travel slightly longer than light travelling along the axis of the fiber, the light is said to be propagating in a higher-order **mode** through the fiber. Fibers with many possible modes are called multimode fibers. Light guided through the core has low attenuation; the light propagates in so called **transmission modes** (Figure 18). However, the transmission modes are to a certain degree affected by the attenuation in the cladding due to the Goos-Hänchen shift which allows the light to penetrate into the cladding at total internal reflection²⁹. Light that is partly or entirely guided through the cladding are **leaky modes** and the attenuation in those modes are significant. Depending on the material composition of the core and cladding light is attenuated at certain wavelengths, which affects the color appearance of the output light.

In some cases the wavelength dependent attenuation varies with the mode, which results in a color shift in the outskirts of the illuminated area²⁵.

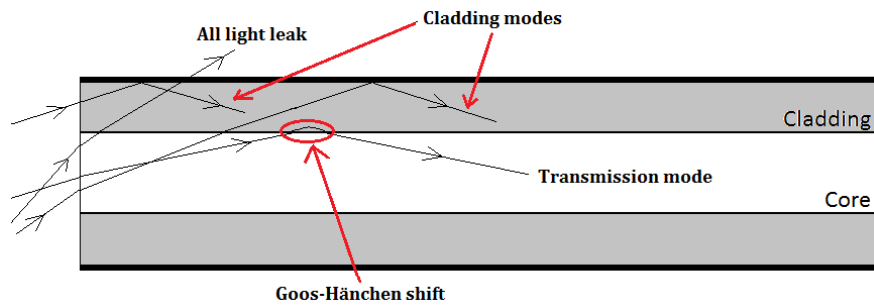


Figure 18. The figure illustrates different kinds of modes in an optical fiber. In the transmission modes light are guided through the core. Other modes where the attenuation is significant are categorized as leaky modes, like the cladding modes illustrated above.

3.2 SP3 solar light system

The SP3 system examined in this study is the third generation of fiber optic solar light systems from Parans. The first system; SP1, was patented in 2004. The later systems, the SP2 and SP3 systems are illustrated in Figure 19. The main difference from previous systems is the ability to track the sun every hour of the day. Stepper motors enable the collector to tilt between 0° and 180° and rotate 360° around its vertical axis. At the startup of the system the collector scans the sky in rectangles of increasing size until a light sensor detects the position of the sun. The collector learns the sun path and catches the sun as it rises the next day.

The collector consists of 36 Fresnel lenses (6.5 cm x 6.5 cm) made of silicone imprinted onto the inside of the glass panel in front of the collector. The lenses are of lower quality but compensated by a significantly lower price than the lenses used in the previous generation; the SP2 system. Consequently the system has 36 fibers, one coupled to each lens. Plastic optical fibers (POF) of doped PMMA are used with a core diameter of 1 mm and are combined into bundles of six according to the arrangement in Figure 10. A glass fiber has lower attenuation and the color properties are better preserved through the fiber. POF is, on the other hand, cheaper and more flexible due to lower bending radius and are therefore used in the SP3 system. At the test site the length of the POF:s was 10 m, but data from a 20 m POF system installed for a parallel project were available for comparative studies. Two different luminaires can be ordered together with the system; The L1 diffuser or the L3 focusing spot³⁰. In this study the latter is used (See section 4.2.6).

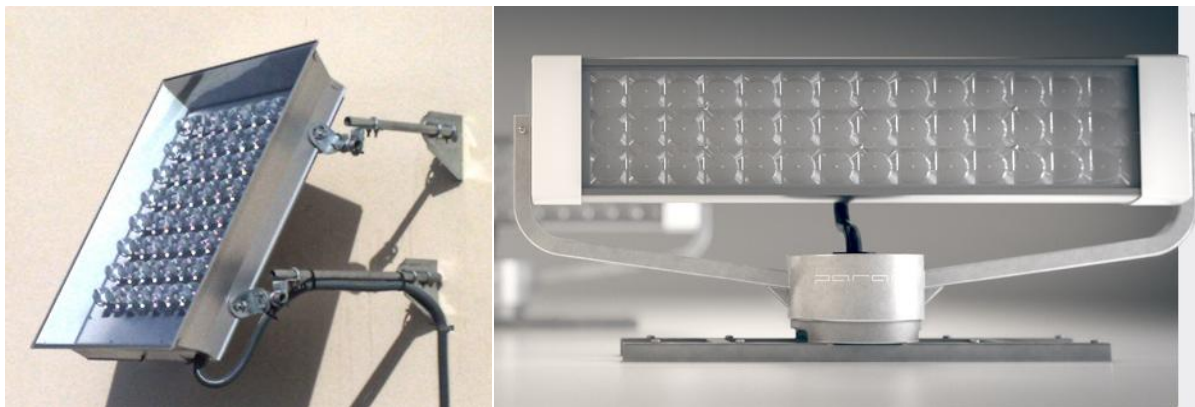


Figure 19. The SP2 system (left) and the SP3 system (right). Retrieved from www.parans.com 2012-08-31.

3.3 Himawari solar lighting system

The Japanese company *La Fôret Engineering Company, LTD* provides a series of SLS systems called *Himawari solar lighting system*. The company has delivered SLS since 1979. The luminous flux output of their products range from 3 840 lm to 63 360 lm. The main distinction from the SP3 system is the fiber material, which for the Himawari systems is of glass³¹.

3.4 TR5-1 solar light system

American Sunlight Direct LLC supplies an SLS named TR5-1 with thicker PMMA fibers than in the SP3 system. The core diameter of the fibers is 3 mm. The system consists of 128 Fresnel lenses. In the previous design the sun was focused by a parabolic reflector onto a secondary reflector which only reflected the visible part of the spectrum into a fiber bundle. This technique has been abandoned in favor of the Parans-like lens array system^{32,33}.

4 Methods

The characterization of the system was done with respect to the optical properties of the components; the Fresnel lens, the filter and the optical fiber, and with respect to the system properties; the illuminance level and spatial light distribution at the test site, the luminous flux output and color quality of the solar light. First the equipment used for the required measurements are presented, then the procedures of the component characterization. After that the test site is described and the way the system was characterized. Finally the tests for optimizing the light balancing are described.

4.1 Experimental methods

4.1.1 Laboratory sun tracker (for single fiber)

To test the coupling capacity of different lenses and fibers a custom built laboratory sun tracker was used (Figure 20). As for a solar fiber optic lighting system, the sunlight is focused into the input fiber end by a lens. No filter was used in front of the fiber end though. Instead the sunlight passes an IR-filter in front of the lens. The filter protected the POF and the glue between the connector and fiber from heat damage. A light sensor tracked the sun and step motors forced the laboratory sun tracker to face the sun. An x-y-z translator made it possible to adjust the position of the fiber input end to maximize the light coupling. The light output of the fibers was later measured using the techniques described in chapter 4.1.2-4.1.3.

4.1.2 Own Manufactured Integrating Sphere

An Own Manufactured Integrating Sphere (OMIS) was used to measure the luminous flux from the output end of a fiber or fiber bundle (Figure 21). The OMIS was calibrated at the SP Technical Research Institute of Sweden in March 2012. The fiber output end was inserted as described in Figure 22 and a Hagner E4-X luxmeter (Figure 22) measured the illuminance at a point next to the inlet of the fiber. A conversion factor determined at the calibration, translates measured illuminance to luminous flux. The OMIS was also used to find the optimum coupling of the solar light when using the laboratory sun tracker by adjusting the position of the input end of the single fiber or bundle until the highest value on the luxmeter was read.

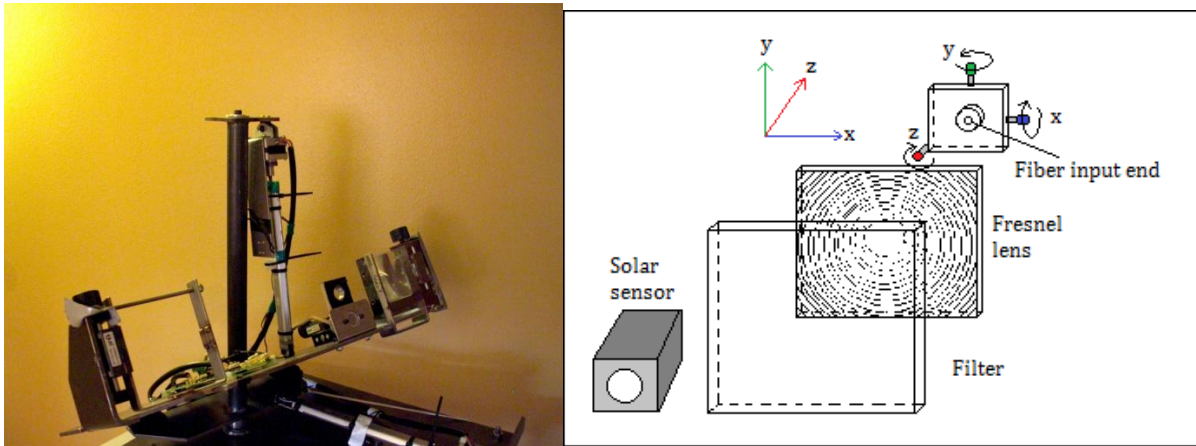


Figure 20. The custom built laboratory sun tracker for fiber and lens tests (left). To the right the principle of the tracker. The light sensor tracks the sun so that the filter, lens and fiber input end become perpendicular to the sun beams.

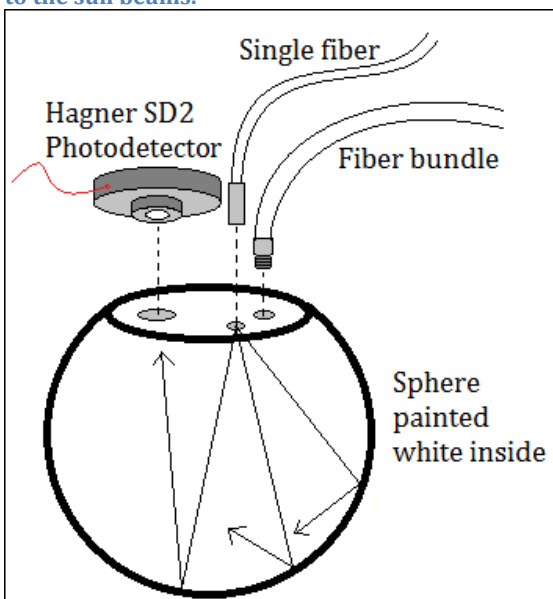


Figure 21. The OMIS. If a single fibre or bundle was measured different inlets were used. The signal was measured in lx by the SD2 photodetector of the Hagner E4-X, and transformed into luminous flux via correction factors.



Figure 22. The Hagner E4-X illuminance meter is equipped with a V-lambda filter for adaption of the human eye and a cosine filter to compensate for the incidence.

4.1.3 SPD measurements

The SPD was determined using an Optical Spectrometric Multichannel Analyzer or more commonly denoted as an optical spectrum analyzer (OSA, Figure 23). It is provided by SI Spectroscopy Instruments GmbH and consist of a detector (Princeton instruments Inc, model EIRY-1024/L), a monochromator (Jarrel-Ash, model JA-150), a gas flow controller (Kobold, model GSU) and a detector controller (Spectroscopy Instruments GmbH, model ST-100). The detector was cooled by Ar-gas. It measures the relative intensity $E(\lambda)$ in the spectrum of 100 - 1165 nm divided into 1024 equal steps, but is only calibrated for the spectrum of 200-900 nm. Color calculations were only performed in the visual spectrum of 380-780 nm that corresponds to the methods setup by CIE¹⁹. The measured intensities were collected and treated in Microsoft Excel 2007 in steps of 1 nm in the spectrum of 380-780 nm and adapted to the CIE 1931 photopic vision (Figure 3). The Correlated Color Temperature (CCT) and Color Rendering Index (CRI) were calculated as described in chapter 2.2.

It was possible to measure the SPD at detection angles of 0°, 15° and 30° of the light. The angle was set using a *black box* (Figure 23) covered inside with non-fluorescent velvet. The black box also limited background noise when measuring the samples, even though a background measurement was made to subtract from the measurement for each sample according to;

$$E_{sample,real}(\lambda) = E_{sample,meas.}(\lambda) - E_{background}(\lambda) \quad (9)$$

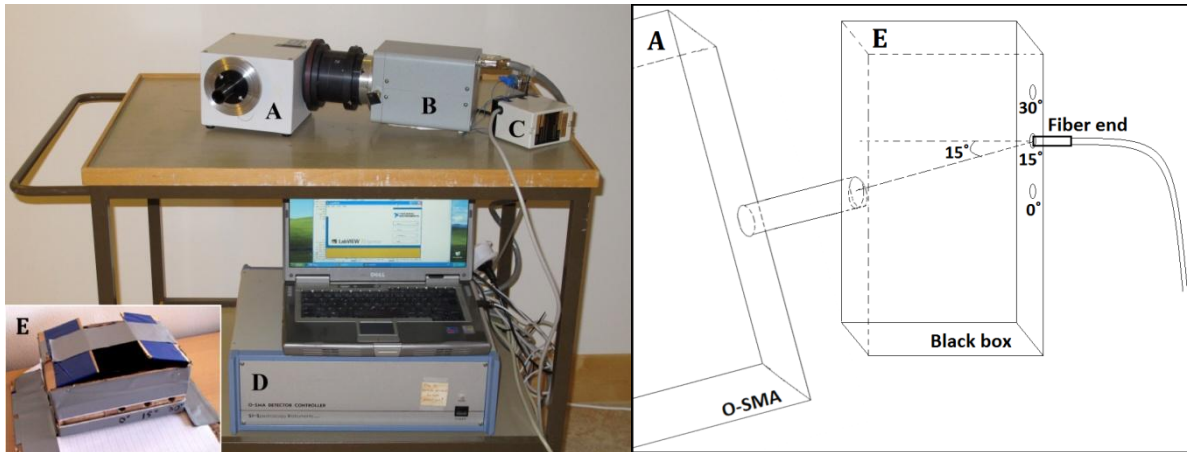


Figure 23. To the left the optical spectrum analyzer consisting of monochromator (A), detector (B), gas controller (C), detector controller (D) and own manufactured black box (E). The latter was used for background noise reduction and ease of measuring the SPD of different detection angles. To the right the work principle of the black box is illustrated.

4.1.4 Transmittance, reflectance and absorbance

The transmittance spectra, $T(\lambda)$, of the system components were studied using an laboratory spectrophotometer; the wavelength was scanned across the selected interval using a grating monochromator and guided through the test sample onto a detector (Figure 24). An optical chopper reduced the background noise. A lock-in amplifier gave information of the frequency of the chopper to the detector. Adjustable irises narrowed the light beam and a microscope objective focused the light. The focusing was especially important when testing an optical fiber in order to couple the light efficiently. The attenuation per meter for a fiber could be determined by the cutback method, for which two measurements are performed; the first with a preferably long fiber, the fiber is then cleaved, leaving only 2 m of the fiber with the input end still in its holder and the second measurement is done. If cutting the fiber is not possible or desirable the second measurement (the reference) was made without the fiber directly after the fiber measurement, keeping all other settings constant. In a paper of Nostell et al. (1999) more details of the laboratory spectrophotometer are given³⁴.

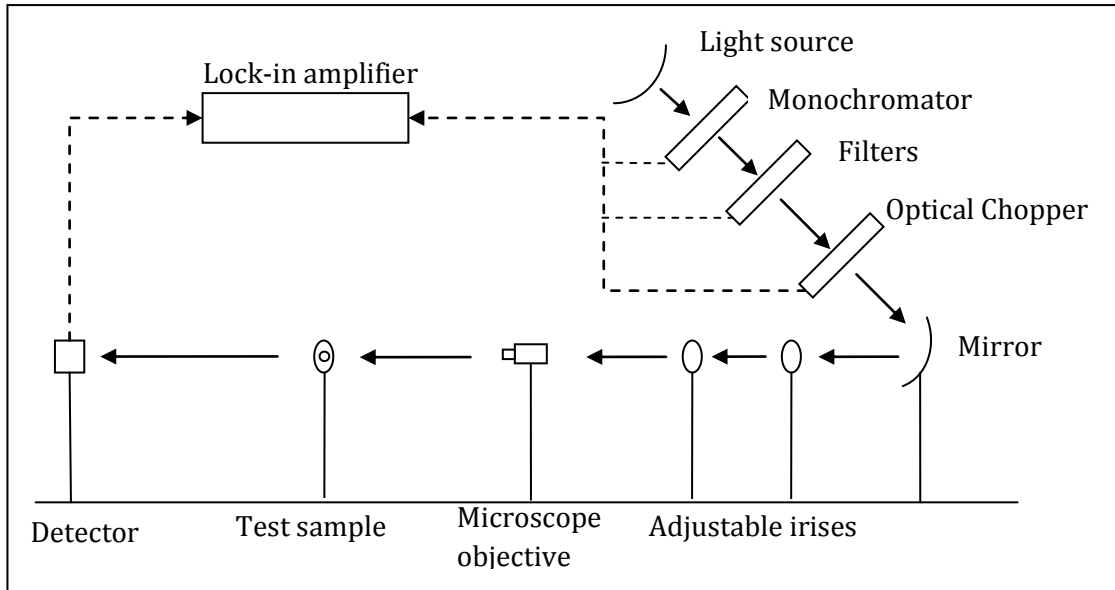


Figure 24. The figure describes the setup of the laboratory spectrophotometer tests schematically. The solid arrows demonstrate the light beam path. The dashed arrows illustrate the signal path from the chopper to the detector via the lock-in amplifier.

The reflectance, $R(\lambda)$, was measured in a Lambda 900 spectrometer from PerkinElmer Inc.

The absorbance $A(\lambda)$ could be calculated as;

$$A(\lambda) = 1 - T(\lambda) - R(\lambda) \quad (10)$$

The attenuation coefficient α in an optical fiber is expressed in dB/km and can be calculated as;

$$\alpha = -\frac{1}{L} 10 \cdot \log_{10}(T) \quad (11)$$

where T is the total transmittance of the fiber and L the length of the fiber in km.

4.1.5 Characterization of the SP3 system components

The following components of the SP3 system were characterized in this study;

- Fresnel lens
- Filter
- Optical fiber

4.1.5.1 The Fresnel lens

The performance of the Fresnel lens of the SP3 system was characterized with respect to the focal length and size and shape of the focal spot. For the required measurements the laboratory suntracker, Own Manufactured Integrative Sphere (OMIS) and optical spectrum analyzer were used. A graded translator of 20 micron steps was used in the x-direction (Figure 20). A 5 m long glass fiber with a core diameter of 200 μm and numerical aperture of 0.43 was used as a probe. When maximum intensity was found via the OMIS, the spectrum was measured by the optical spectrum analyzer in light detection angles of 0° and 15° respectively using the black box (Figure 23). The fiber input end was moved and the spectrum measurements were repeated at 0° for the FWHM (Full Width at Half Maximum) and the double FWHM (Figure 36). Because of pincushion distortion, a common lens problem for square shaped lenses, where the magnification around the optical axis is greater than on the axis, the FWHM varies depending on which direction the probe is moved²⁴. The pincushion distortion that was observed for the SP3 lens is illustrated in Figure 25. The FWHM along one of the four arms would also be interesting to assess but is omitted in this study. The FWHM was only sought in the x-direction.

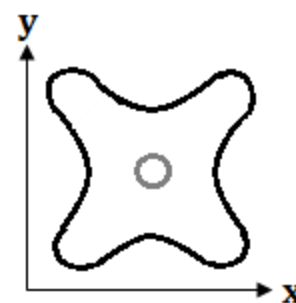


Figure 25. Pincushion distortion observed for the SP3 lens.

The Fresnel lens is a silicone pattern stamped onto a glass plate. The transmittance spectrum of the glass plate inclusive and exclusive of the silicone was determined using the laboratory spectrophotometer (Figure 24).

4.1.5.2 The Filter

The ability of the filter to separate the UV and NIR light was determined by transmittance and reflectance measurements using the laboratory spectrophotometer and Lambda 900 respectively.

4.1.5.3 The Plastic optical fiber

The plastic optical fiber (POF) was characterized with respect to the transmittance using the laboratory spectrophotometer (Figure 24). The angle dependency was performed by moving the detector in a quarter of a circle in steps of 5° (Figure 26). Because of the symmetry of the spatial distribution of the light through the POF measurements in a quarter of a circle are sufficient.

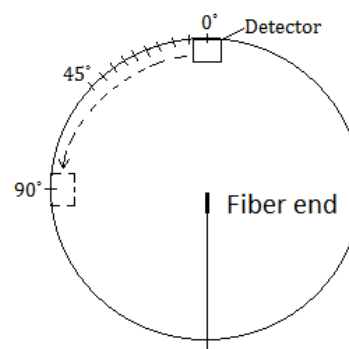


Figure 26. The light intensity in different angles was measured by moving the detector in a quarter circle.

4.2 The setup of the test site

4.2.1 Location

The test site is located at the Ångström Laboratory in Uppsala, Sweden.

4.2.2 Activity in the test site

The test site has not been set up for the examination of the SP3 solar lightning system specifically. The room has been there and filled the same purpose since the Ångström laboratory was built in 1995. The room can be divided into two areas of different functions. The first area lies next to elevator shafts and works as a hall way. The second area, in the east part of the test site works as a study environment for students. In the study area the solar light luminaires are installed marked with red dots in Figure 28. According to the standard EN 12464-1:2011 the hallway should be illuminated by 100 lx minimum at 85 cm above the floor. For reading tasks, the corresponding illuminance level is 500 lx¹⁷. However, the illuminance level in the study area, where students are reading, before the installation of the solar light system was about 300 lx.

4.2.3 Dimensions

The test site is illustrated in Figure 28 below. The height of the test site is 2.50 m. A window in the south east corner gives daylight to the table next to the window. Therefore the solar luminaires are offset to the north part of the study area. Figure 28 also gives information about the positions of the different luminaires and where illuminance measurements were performed (cross points of dashed lines).

4.2.4 The test site in DIALux

The test site was drawn using the CAD software DIALux (v 4.10) developed for planning indoor lightning. The software was used for two reasons; initially it was meant to illustrate the test site, but later it turned out to be a tool for simulating different light scenes in the test site depending on the illuminance from the sun. In this way measured results can be compared with simulated light scenes verifying the setup of the test site in DIALux, and thereafter predictions can be made through simulations. Screen shots from the DIALux software can be seen in section 5.2.3. For illustrating the illumination distribution in the test site for a certain measurement series the performance of the artificial luminaires as well as the solar luminaires was set as input data. The date, time of the day and weather (sunny or cloudy) was set according to measurement series to match the light distribution from the window. The DIALux simulation could be matched with the real measured illumination distribution by changing the retention factors of the luminaires. In this way it is possible to rearrange the luminaires in DIALux in order to optimize the usage of the luminaires.

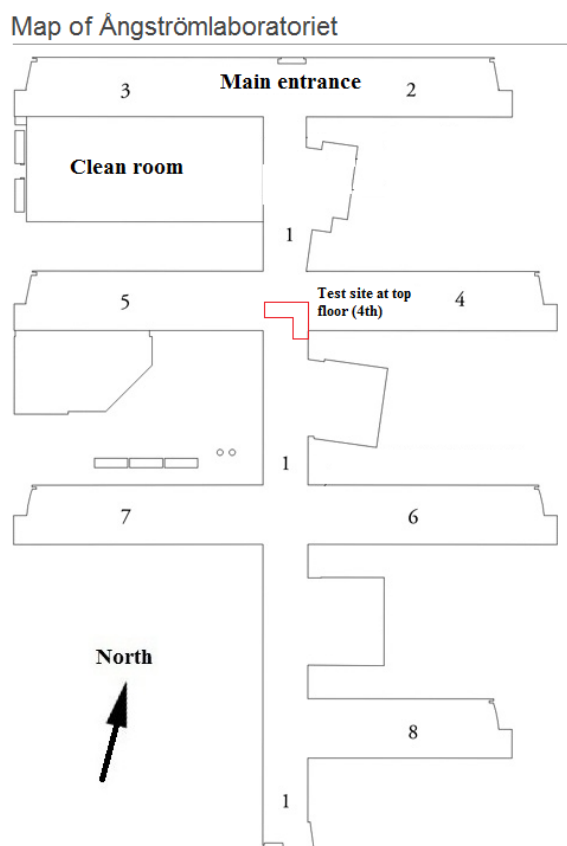


Figure 27. The Ångström laboratory. The red L-shaped figure marks the location of the test site. The building is four floors high and the test site is located on the top floor.

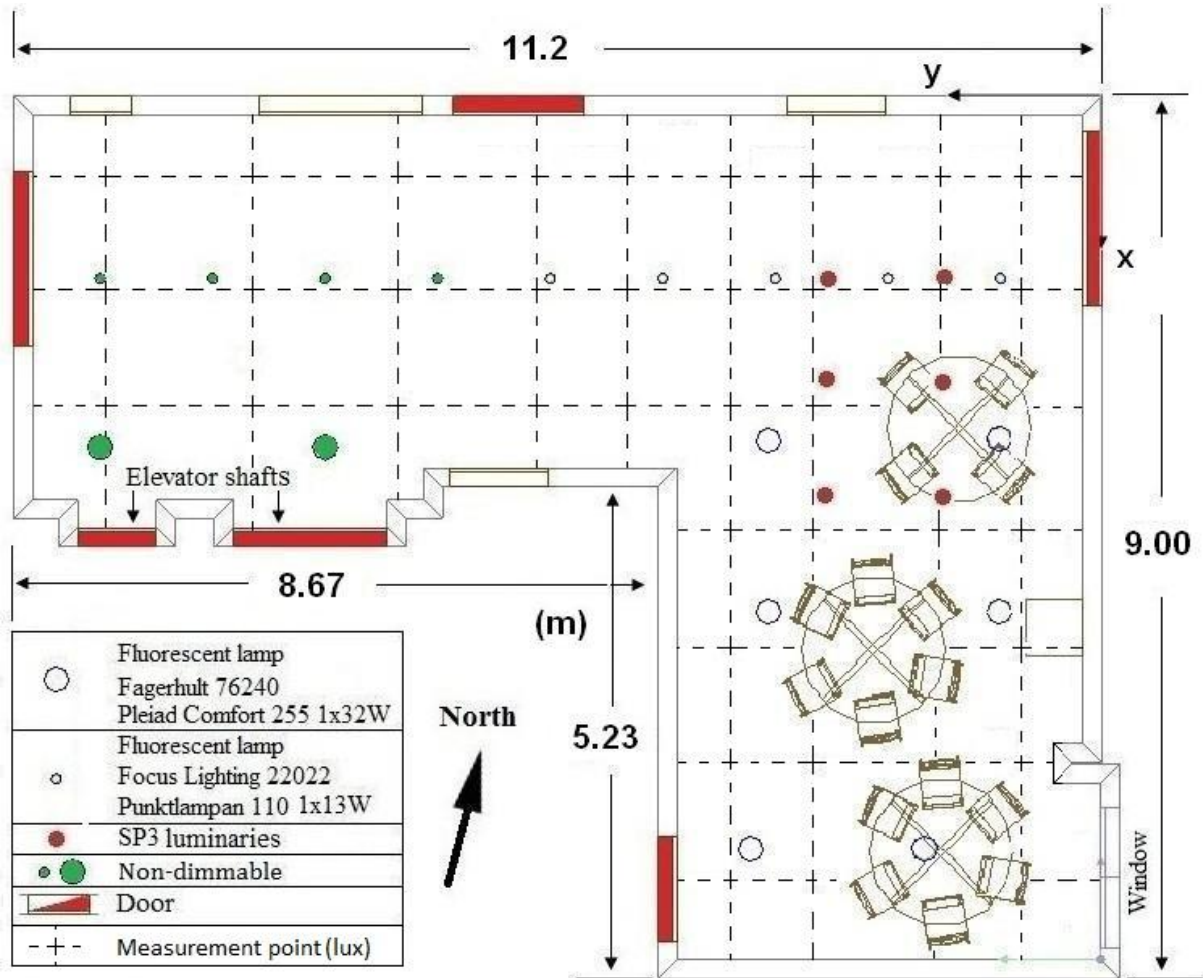


Figure 28. The test site at the Ångström laboratory. Red marked doors are leading to adjacent departments or hall ways and are heavily trafficked during working hours. Green marked artificial light are not dimmable. At the cross points of the dashed lines the illuminance was measured at workplane (85 cm above the floor).

4.2.5 Materials

The characteristics of the material in the test site are presented in Table 1. The reflection factors are estimated according to standards in DIALux.

Table 1. The estimated reflection factors of the walls, ceiling and floor of the test site used in DIALux simulations. Also presented is the estimated transmission factor of the window.

Element	Material	Reflection factor
Walls	White polish	0.70
Ceiling	White Ceiling panels (60 x 60 cm)	0.70
Floor	Linoleum	0.35
Window	Coated double glass*	0.75 (Transmission)

*Two Shcott Pyran S® 6 mm panes of individual transmission factor of 0.9. Including the coating the total transmission factor for the window is estimated to 0.75.

4.2.6 Luminaires

For each type of luminaires at the test site, technical data were provided from the manufacturer in form of a eulumdat file (.ldt). It contains the luminous flux output, the power consumption and most importantly the spatial light distribution of the luminaire. The eulumdat file is used when placing the luminaires in the DIALux model.

4.2.6.1 Artificial luminaires

There are two types of down light electrical luminaires in use at the test site. These are presented in Figure 29 along with technical data and light distribution. Both are high frequency luminaires. The efficacy was calculated from the specified power consumption and luminous flux output of the two luminaires.

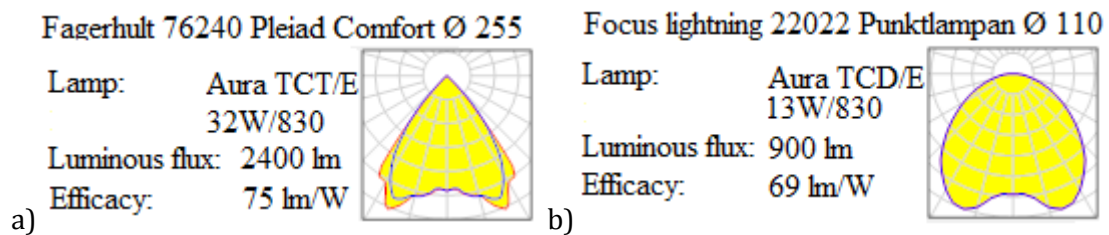


Figure 29. Technical data for a) Fagerhult 7640 Pleiad Comfort 255 and b) Focus lightning 22022 Punktlampan Ø 110.

4.2.6.2 Parans solar light luminaires

The luminous flux from the Parans solar luminaires depends on the direct visible illuminance of the sun. When the system was newly installed the luminous flux from each solar luminaire was measured using the own manufactured integrating sphere (OMIS, Figure 21) and the Hagner EX-4 luxmeter (Figure 22). Figure 30 illustrates the performance of the SP3 luminaires with and without the L3 spot. The luminous flux and power consumption is due to the product specification of the SP3 system at 100 klx direct sun illuminance and 10 m cable of six optical fibers³⁰. The efficacy is calculated from those specifications. The efficacy of the solar luminaires is significantly higher than for the artificial light sources.

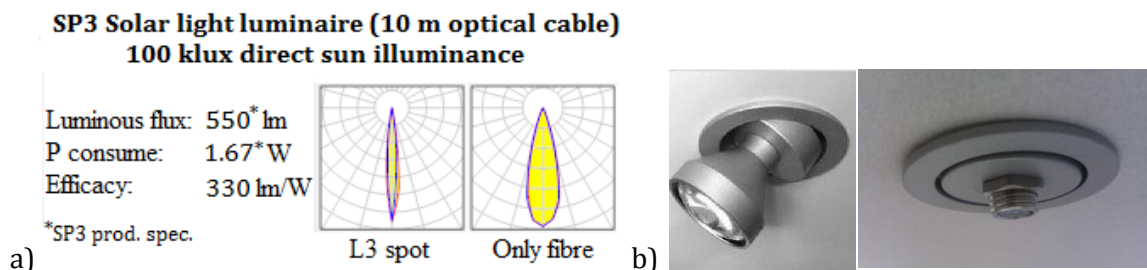


Figure 30. a) Technical data and polar diagrams of a SP3 solar light luminaire with and without the L3 spot and b) The solar light luminaires with and without the L3 spot.



Figure 31. The output light distribution obtained from the L3 spot luminaires (left) and directly from the fiber ends (right). The table seen in the left picture was used for illuminance measurements at the test site at 85 cm above the floor.

4.2.7 Characterization of the SP3 system

4.2.7.1 Luminous flux of the system

The luminous flux was measured repeatedly at different weather conditions using the OMIS in combination with the Hagner luxmeter.

4.2.7.2 Spatial distribution of the solar light

The spatial distribution of the solar light was determined by moving the Hagner luxmeter starting from nadir at workplane (85 cm above the floor) in steps of 2.5 cm until no change in illuminance was noted. The contribution from the surrounding light sources was measured when the solar luminaire was covered and subtracted from the illuminance. The spatial distribution was determined with and without the L3 spot.

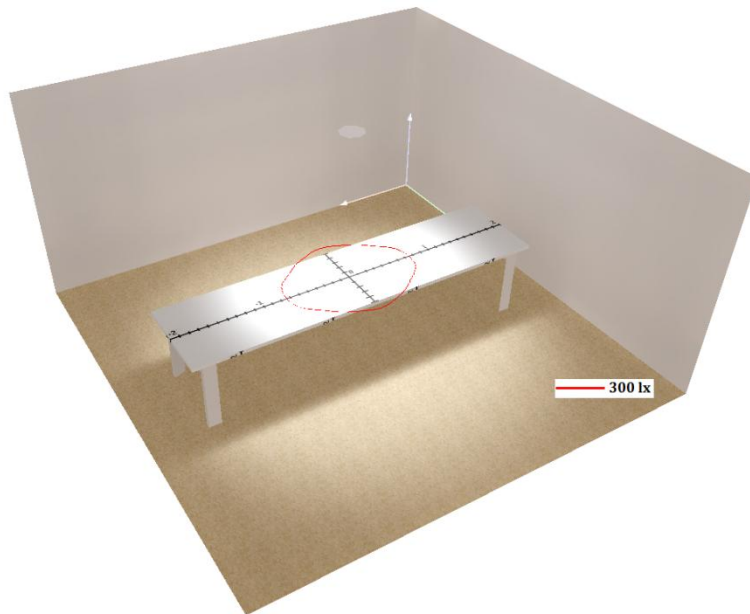


Figure 32. The testroom in DIALux.

To study the correlation between the spatial intensity distributions simulated in DIALux and real measured data, a test room was created in DIALux; 5 m x 5 m and 2.5 m high. In the center of the room a table was placed, with its table top in the workplane (85 cm above the floor). The table top surface was graded with steps of 1 dm (Figure 32). The isophote (line of constant illuminance) at the workplane was shifted manually by changing the illuminance level in order to find the cross point in each real measurement position (0 cm, 2.5 cm, 5 cm...). In Figure 32 this is exemplified; the isophote crosses the graded bar on the table 8 dm from nadir, when the illuminance was set to 300 lx.

4.2.7.3 Illuminance at the test site

Illuminance measurements were performed on a 0.85 m distance above the floor in a grid network as illustrated by the dashed lines in Figure 28. The Hagner luxmeter was placed on a moveable table (Figure 31). The grid network is not symmetrically along the x-axis. The reason is obstacles along north horizontal line.

4.2.7.4 The color of the solar light

The spectra of the solar luminaires were measured by the optical spectrum analyzer. From those the correlated color temperature (CCT) and the color rendering index (CRI) could be calculated according to the methods described in chapter 2.2.

4.2.8 Survey for evaluation of the lighting environment by the students

In addition to the technically determined quality of the light discussed earlier, a questionnaire was available for the students to fill in at the test site. The questionnaire had 18 questions and has been used in previous studies³⁵. Thorbjörn Laike from Lund University was familiar with the questionnaire in his work and the analysis of the answers was performed in collaboration with him. The questionnaire is in Swedish and can be found in Appendix A.

4.2.9 Balancing of the artificial light

One of the targets of this study was to find an efficient method to balance the solar light and artificial light at the test site. Studies in laboratory environments have been done previously³⁶. In this study though, a real location for a solar light system was evaluated and similar studies are harder to find in the literature, which makes this study unique.

The regulation of the artificial light at the test site requires a proper control signal. Different sensors were installed in the test site and their ability to balance the light was examined. Figure 33 shows the different sensors and their position at the test site. The numbers correspond to the sensor IDs in the table in the bottom right corner.

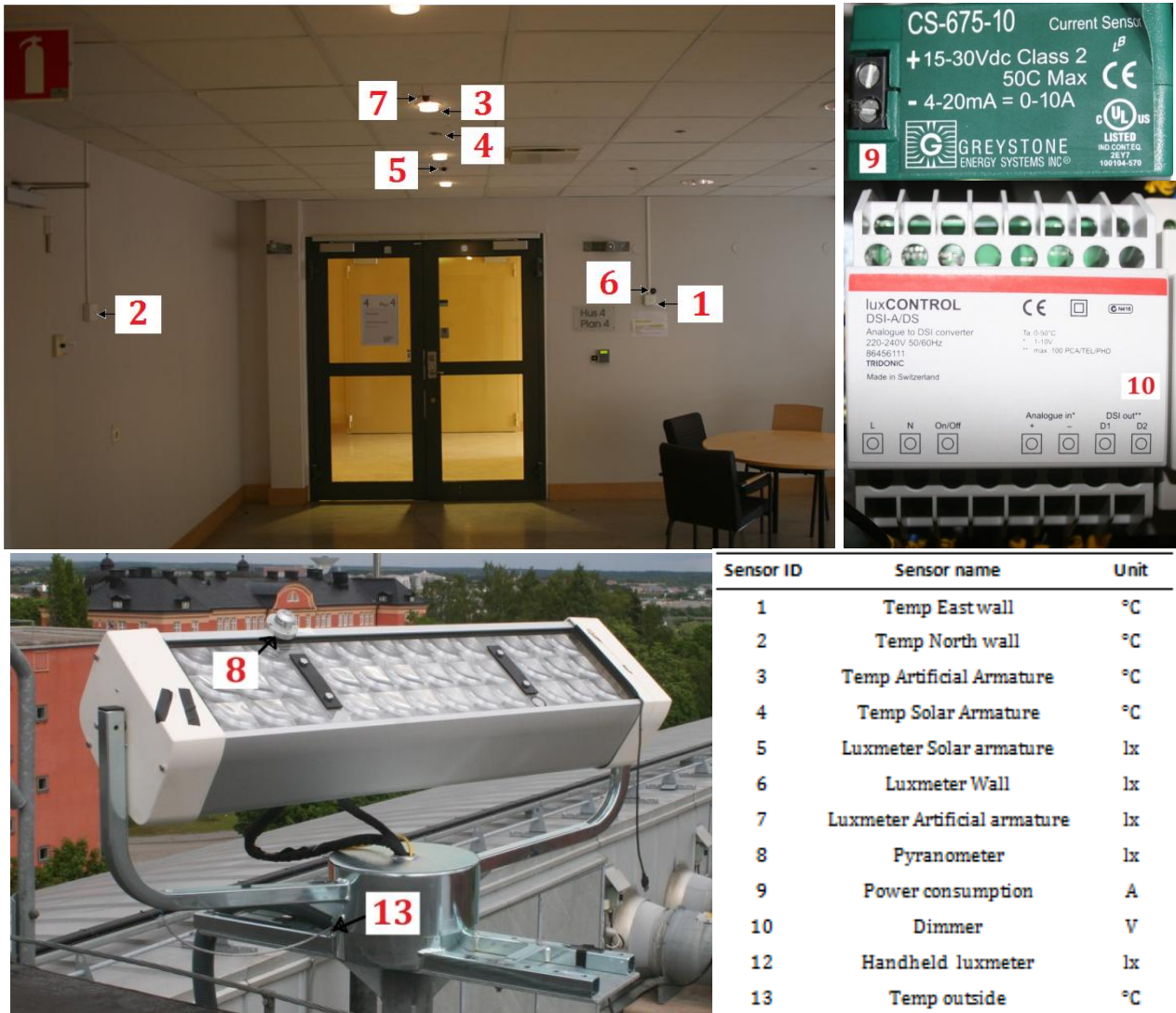


Figure 33. The pictures show where the sensors were placed at the test site. The marked numbers correspond to the Sensor IDs in the table.

Different approaches of controlling the artificial light in solar light systems have been investigated in earlier studies. In this study, three methods were examined;

1. Pyranometer measuring the global horizontal illuminance.
2. Pyranometer attached to the SP3 collector measuring the direct sun illuminance.
3. Indoor light sensors at the test site.

The first method has been tested in previously for the earlier SP2 system of Parans (Figure 19)³⁷.

Figure 34 shows the relation between the illuminance under the solar light luminaires (internal illuminance) and the global horizontal illuminance measured outside (external illuminance). As can be seen the correlation is poor. The authors suggest it might depend on the fact that the solar lighting system only couples the direct sun illuminance efficiently but the pyranometer measures the global illuminance, hence the balancing of the artificial light will be problematic using this method. The direct sun illuminance component cannot be calculated from measured irradiance of any static pyranometer.

In this study, for the second method, a pyranometer (Kipp & Zonen SP Lite 2) were attached to the SP3 collector as shown in Figure 33, sensor ID 8. Three different approaches were examined; (1) the pyranometer was used as it is, (2) a tube, designed with the same numerical aperture (0.5) as the fibers, was attached around the sensor, (3) on top of the tube a filter (NT 64-460, Edmund Optics, Inc.) was placed to limit the UV and NIR parts of the light. Figure 35 illustrates the three different setups.

In the third method the three indoor illuminance sensors were used for balancing the light level at the test site. A PID regulator with constant setpoint as control signal was used for each sensor. The sensors were placed beside an artificial luminaire, a solar luminaire and on the wall (Figure 33, sensor ID 7, 5 and 6 respectively).

4.2.10 Energy consumption

The energy consumption of the solar light system was measured using a Voltcraft Energy Logger 4000. The total energy consumption of all loads at the test site; the artificial lights, the sensors, the web logger and the SP3 system was logged by the transformer (Figure 33, sensor ID 9). Because the tests ran only over a few months the annual energy consumption of the solar light system had to be estimated.

The temperature sensors were used for verifying the hypothesis that the artificial lights produce more heat than the solar luminaires do.

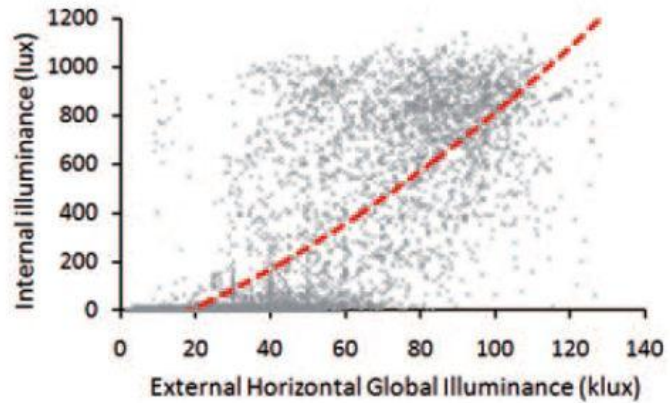


Figure 34. The illuminance under the SP2 armatures as a function of the global horizontal illuminance³⁷.

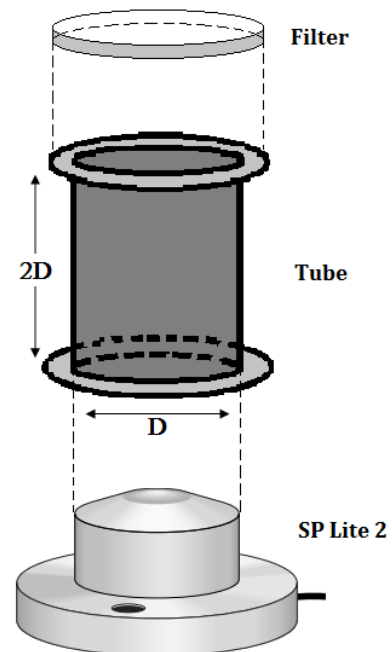


Figure 35. The SP Lite 2 Pyranometer from Kipp & Zonen. For finding an optimal control signal a tube and filter were attached to the pyranometer.

5 Results

5.1 System components

5.1.1 The SP3 Fresnel lens

The focal length of the Fresnel lens was determined to 83 mm. Since the size of the Fresnel lens is 6.5 mm x 6.5 mm this gives the lens a numerical aperture (NA) of 0.36. The intensity as a function of the distance from the center of the focal spot is illustrated in Figure 36. The FWHM and the double FWHM are marked. The red dashed line is a Gaussian fit to the measurement points. Since a 0.2 mm thick glass fiber was used as a probe, the real light intensity distribution curve is 0.2 mm narrower than the measured, which can be realized when studying Figure 37. When the probe has been moved one radius (R) of the focal spot in the x-direction, the probe is still detecting some light. Moving the probe another radius (r) of the probe the light intensity can no longer be detected, thus the real width of the light intensity distribution curve is $2*r$ narrower than the measured.

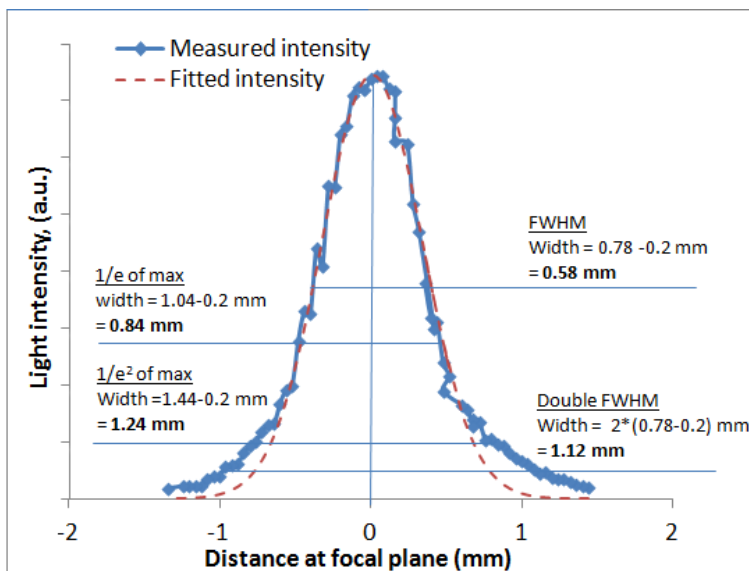


Figure 36. The light intensity distribution across the focal plane for the Fresnel lens.

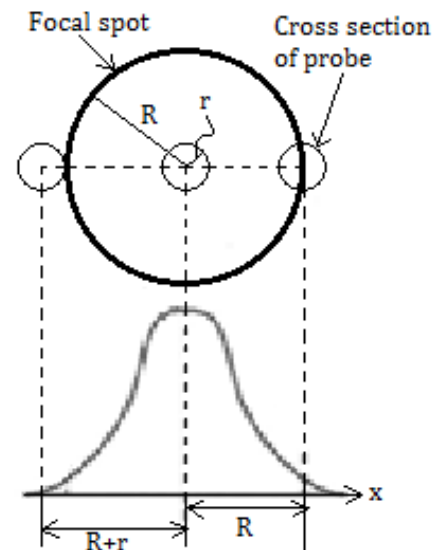


Figure 37. The figure shows that the real intensity distribution of the focal spot is the $2*r$ of the probe narrower than the measured distribution.

The spectral power distribution at maximum intensity (center of focal spot), FWHM and double FWHM were measured using the optical spectrum analyzer and the black box (Figure 23) and are presented in Figure 38, along with their associated correlated color temperature and color rendering index. The slight shift to the left for the SPD curve of the double FWHM relative the other curves are confirmed by the higher correlated color temperature. This might be an effect of chromatic aberration, refracting blue light to the outskirts of the focal spot (see chromatic aberration, Figure 14c and the distribution of the solar light in Figure 31).

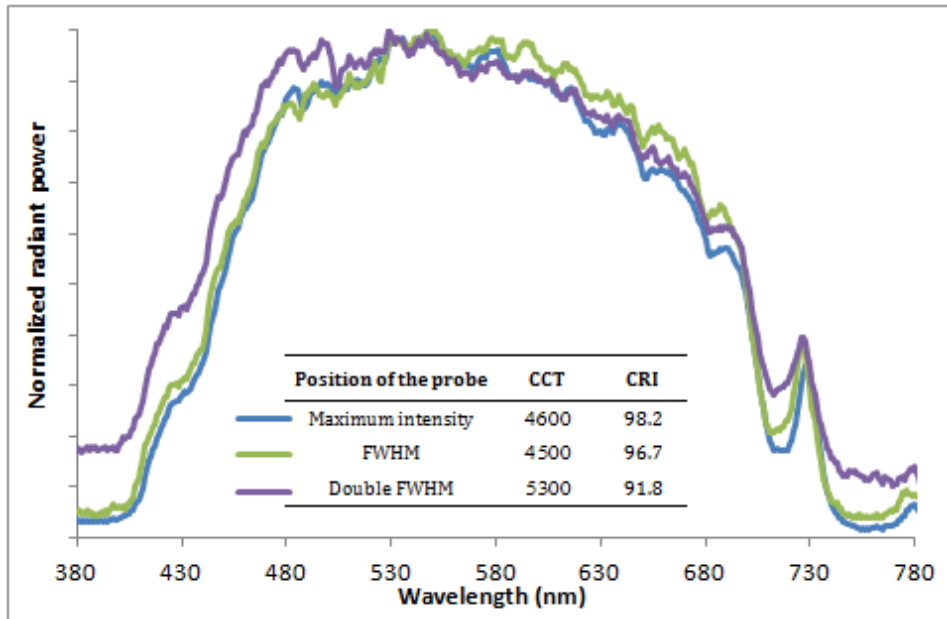


Figure 38. The SPD at the maximum intensity, the FWHM and double FWHM in the focal plane.

The transmittance through the Fresnel lens including the glass plate and only for the glass plate (Figure 39) was measured using the laboratory spectrophotometer (Figure 24). The transmittance is high, about 90 % in VIS, but decreases in NIR for the Fresnel lens.

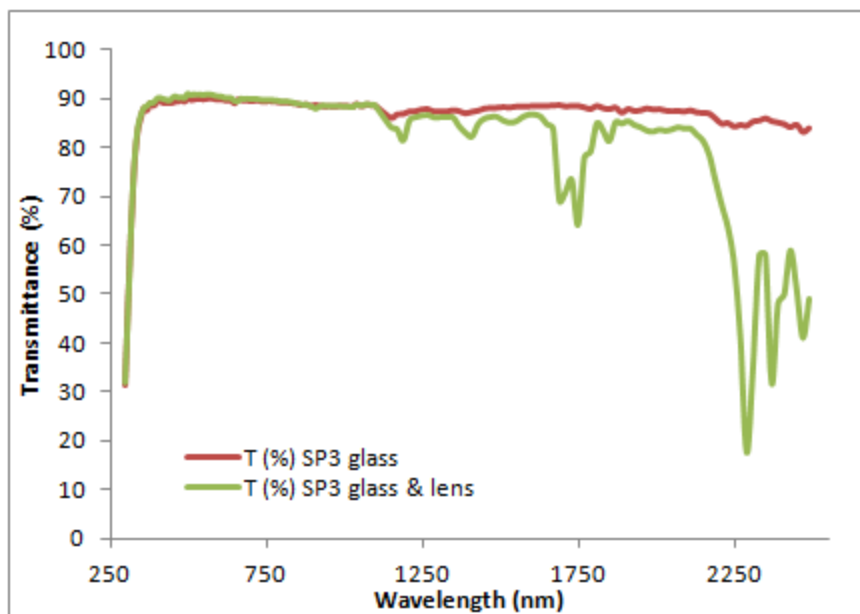


Figure 39. The transmittance through the SP3 collector glass plate inclusive and exclusive the Fresnel lens.

5.1.2 The SP3 Filter

The first filter did not protect the POF from UV and NIR light. It was later substituted. More information about the properties of these filters can be found in a confidential report (T Volotinen, Uppsala University and Daniel Johansson, Parans Solar Lighting AB).

5.1.3 The SP3 POF

The transmittance spectrum in VIS of the SP3 optical fiber is presented in Figure 40. The transmittance dips around 545, 625 nm and 730 nm are expected according to the absorption in the CH-bindings described in Figure 16, pp. 10.

The transmittance through the SP3 POF as a function of the detection angle was measured when focusing the light beam with objective lenses of different NA. However the expected difference in spatial distribution of the light when coupling the light in different angle cones into the fiber could not be seen. This could depend on the piece of glass at the end of the fiber bundle, diffusing the light similar independent of the numerical aperture of the light coupled into the fiber. It could also depend on suboptimal coupling of the light into the fiber.

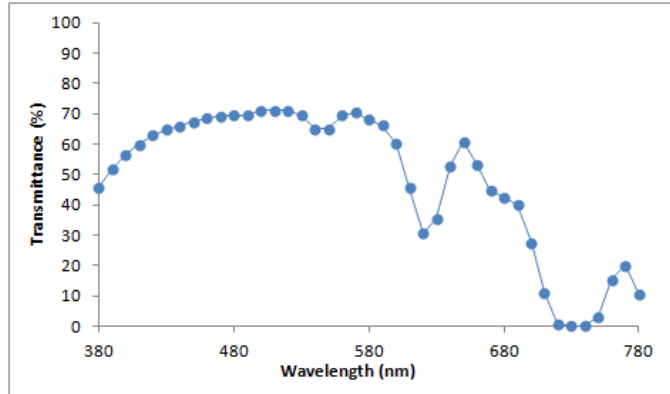


Figure 40. The transmittance through a 10 m SP3 POF. Light is coupled into the fiber using an objective lens of NA 0.1.

5.2 The solar lighting system

5.2.1 Luminous flux

The luminous flux coming out of the solar luminaires was measured at different times of the day and varied sun intensity. The luminous flux as a function of the direct sun illuminance is presented in Figure 41. On a clear day of 130 klx direct sun illuminance the mean luminous flux was 767 (± 33) lm/solar luminaire. At 100 klx the output was approximately 500 lm, which is slightly lower than specified by Parans (550 lm) at the same sun intensity. The luminous flux of the 20 meter system on a clear day of 122 klx was 509 (± 50) lm/solar luminaire and was somewhat higher (400 lm) than specified by Parans (350 lm) at 100 klx direct sun illuminance.

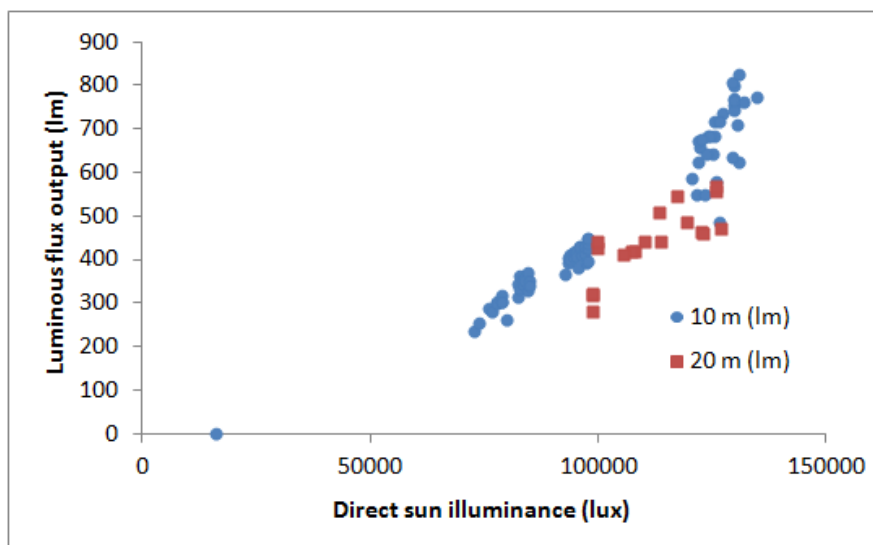


Figure 41. The luminous flux output from solar luminaires of 10 m POF and 20 m POF.

5.2.2 Spatial intensity distribution

The spatial intensity distributions of the solar luminaires without the L3 spot (Figure 30) were significantly wider than Parans specified distribution data modeled in DIALux, which Figure 42a) shows. The measured data were collected during sun conditions of about 125 klx direct sun illuminance. To get the same illuminance at nadir in DIALux as measured the luminous flux of the solar luminaire had to be set to 900 lm instead of the 750 lm that it actually had at that sun condition (Figure 42).

Sensitivity analysis was done by changing the reflection factors of the walls and ceiling from 0.70 to 0, which had no impact on the result, thus the test room in DIALux (Figure 32) used for modeling the spatial distributions of the luminaires was sufficiently large for avoiding reflective contributions.

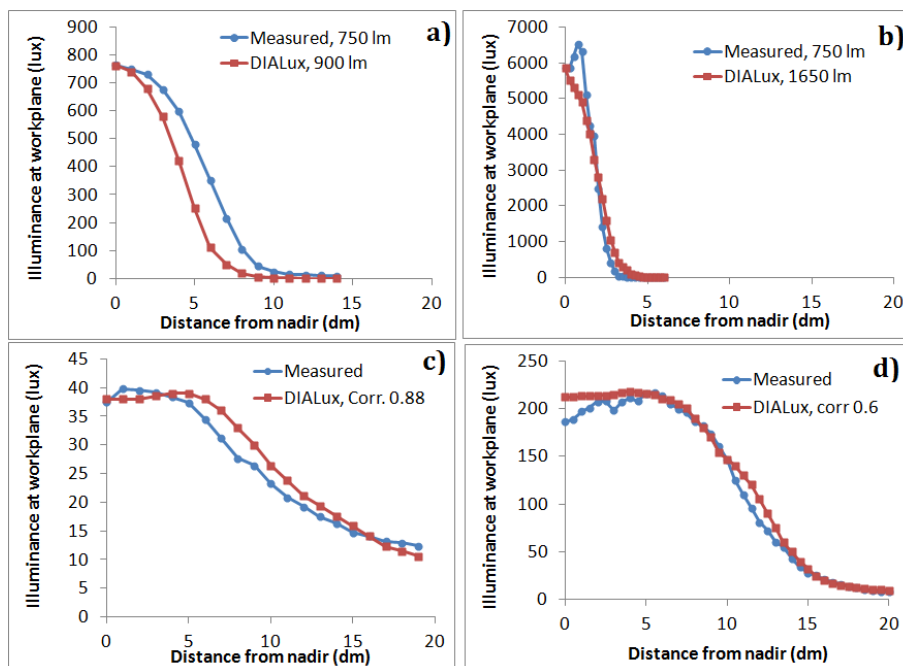


Figure 42. The illuminance at work plane for a) the solar luminaire with bare fiber, b) solar luminaire with L3 spot, c) Focus Lighting 22022 Punktlanpan \varnothing 110 and d) Fagerhult 76240 Comfort Pleiad \varnothing 255. The blue curve represents the measured illuminance at the test site and the red curve represents the simulated illuminance in DIALux.

When using the L3 spot the same illuminance at nadir in DIALux was obtained when setting the luminous flux to 1650 lm (compare 900 without the L3 spot, Figure 42b). The distribution correlation between real data and DIALux model after this “nadir fit” was somewhat better with the L3 spot than without.

For the two artificial luminaires, the luminous flux was adjusted with a correction factor of 0.88 and 0.6 respectively, relative the specification from the manufacturer and high correlation was obtained (Figure 42c-d). A correction factor below 1 is normal due to aging and dirtiness of the luminaires. These luminaires were installed when house 4 of the Ångström Laboratory was built in 2000 and has not been cleaned since then according to a service technician. Notable is that the solar luminaires give a more intensive, but narrower light distribution than the artificial lights and especially with the L3 spot. This implies the development of a method for spreading the solar light more widely. The poor correlation between the DIALux files and real measured data

should be solved by changing the eulumdat-file of the solar luminaires (remeasure the spatial distribution of the solar luminaire in the lab).

The area illuminated by the different luminaires can be calculated from Figure 42. This is done for the illuminance levels recommended for reading tasks (500 lx) and hallways (100 lx). Note that normally these standard levels are reached because of background light from windows and by placing adjacent luminaires close enough to each other. In Table 2 the illuminated area for the solar luminaire is presented, the background light is not accounted. Since the Fagerhult luminaires are installed for reading tasks and are set to give just over 200 lx at nadir (without background), the illuminated areas of >200 lx are also presented in Table 2. The difference between measured illuminated area and simulated in DIALux follows from the differences in Figure 42.

Table 2. The illuminated areas for the solar luminaires with and without the L3 spot and the two artificial lights at the test site are given at three illuminance levels.

Illuminance	> 100 lx		> 200 lx		> 500 lx	
	Measured (m ²)	DIALux (m ²)	Measured (m ²)	DIALux (m ²)	Measured (m ²)	DIALux (m ²)
Luminaire						
SP3 only fiber	2.06	1.17	1.58	0.90	0.84	0.38
SP3 L3	0.31	0.43	0.28	0.44	0.23	0.32
Focus Lighting	0	0	0	0	0	0
Fagerhult	4.08	4.52	1.54	1.77	0	0

5.2.3 Illuminance at the test site

The light distribution at the workplane over the whole test site was measured according to the grid network (Figure 28) for five different weather conditions defined in Table 3. The measured light distribution and the analogous model in DIALux for each condition are presented in Figure 43. The color grades were chosen according to the standard levels described in the previous chapter and also for 300 – 500 lx because this was the illuminance level at the study area before the solar lighting system was installed (Figure 43a). The luminous flux of the luminaires in DIALux was set to fit the illuminance at nadir as described in chapter 5.2.2. The solar luminaires were not equipped with the L3 spot in the distribution measurements presented below.

Table 3. Five illumination configurations at the test site for which the illuminance at workplane was measured and simulated in DIALux.

Config.	Weather	Artificial light	Solar luminaires	Direct sun illuminance (lx)
a)	Cloudy	Off	No contribution	10 000
b)	Cloudy	Max output	No contribution	3 800
c)	Sunny	Max output	Not installed	90 000
d)	Sunny	Fully dimmed	High contribution	112 000

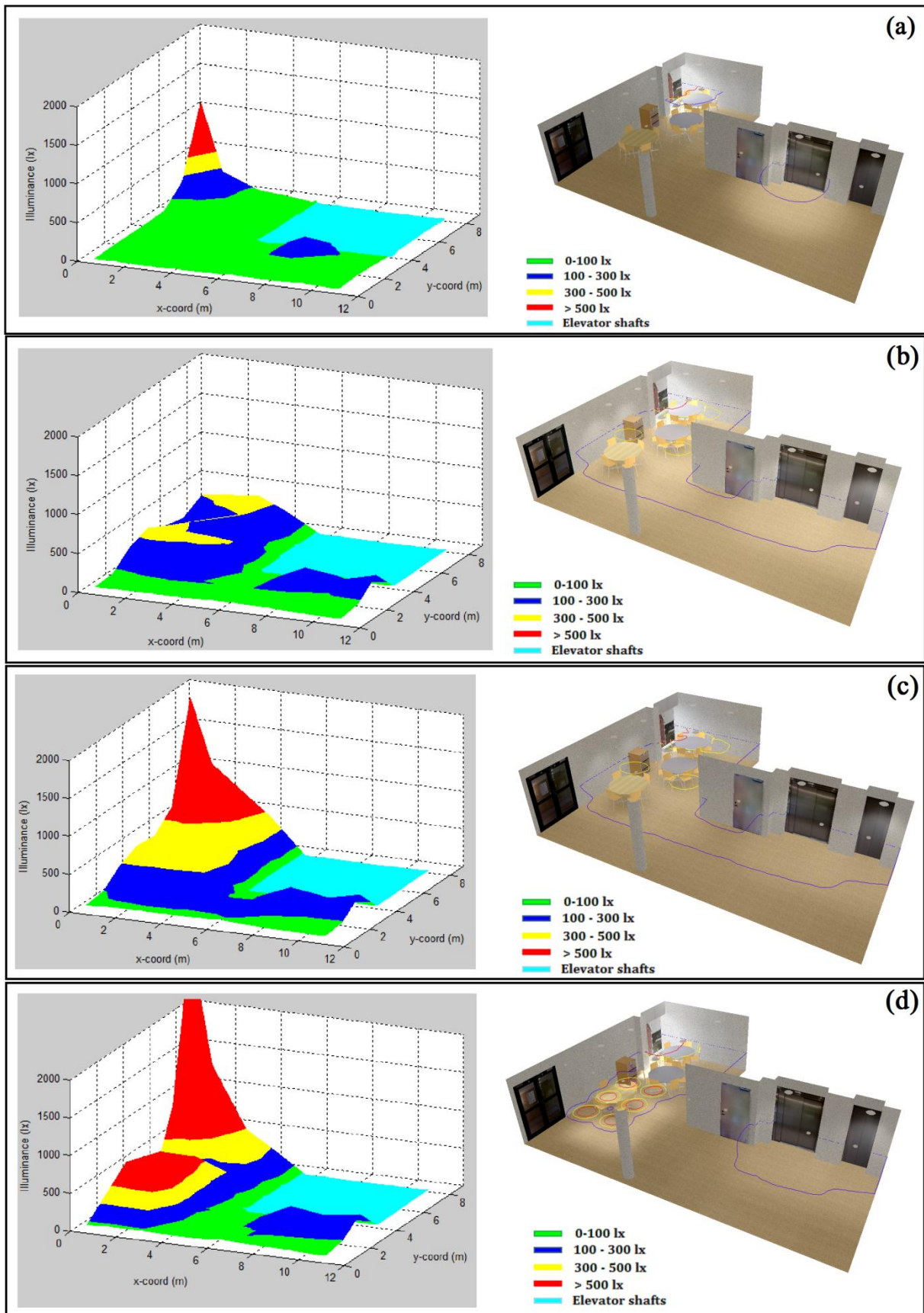


Figure 43. The illuminance at the test for five different illumination configurations, defined in Table 3. To the left the illuminance measured at the test site, and to the right the corresponding simulation in DIALux.

5.2.4 Color of the luminaires

The intensity spectra of the six solar luminaires were measured during sunny conditions. At overcast sky the intensity of the solar luminaires was too low for the optical spectrum analyzer to detect. The spectral power distribution (SPD) curves obtained from these measurements did not vary significantly between the luminaires but small variations due to detection angle and length of the plastic optical fiber (POF) were observed. In Figure 44a the spectral power distribution (SPD) curves of the 10 m SP3 system of 0° and 15° detection angles are presented and also the fluorescent light source in the test site. In Figure 44b the SPD of the 10 m and 20 m SP3 system is presented and in Figure 44c the daylight spectrum can be seen. The correlated color temperature (CCT) and the color rendering index (CRI) of the light sources is presented in Figure 44d.

In the 15° detection angle the SPD curve of the 10 m SP3 system is shifted a little to the right resulting in a warmer light (lower CCT). Hence, the blue light is attenuated more relative other colors in the higher order transmission modes. The transmission dips caused by the properties of the PMMA POF at 625 and 730 nm is stronger relative the general attenuation for the longer fiber system (20 m) as expected. This means that in addition to higher attenuation in a longer fiber system, the color quality of the light is poorer, being less akin to daylight.

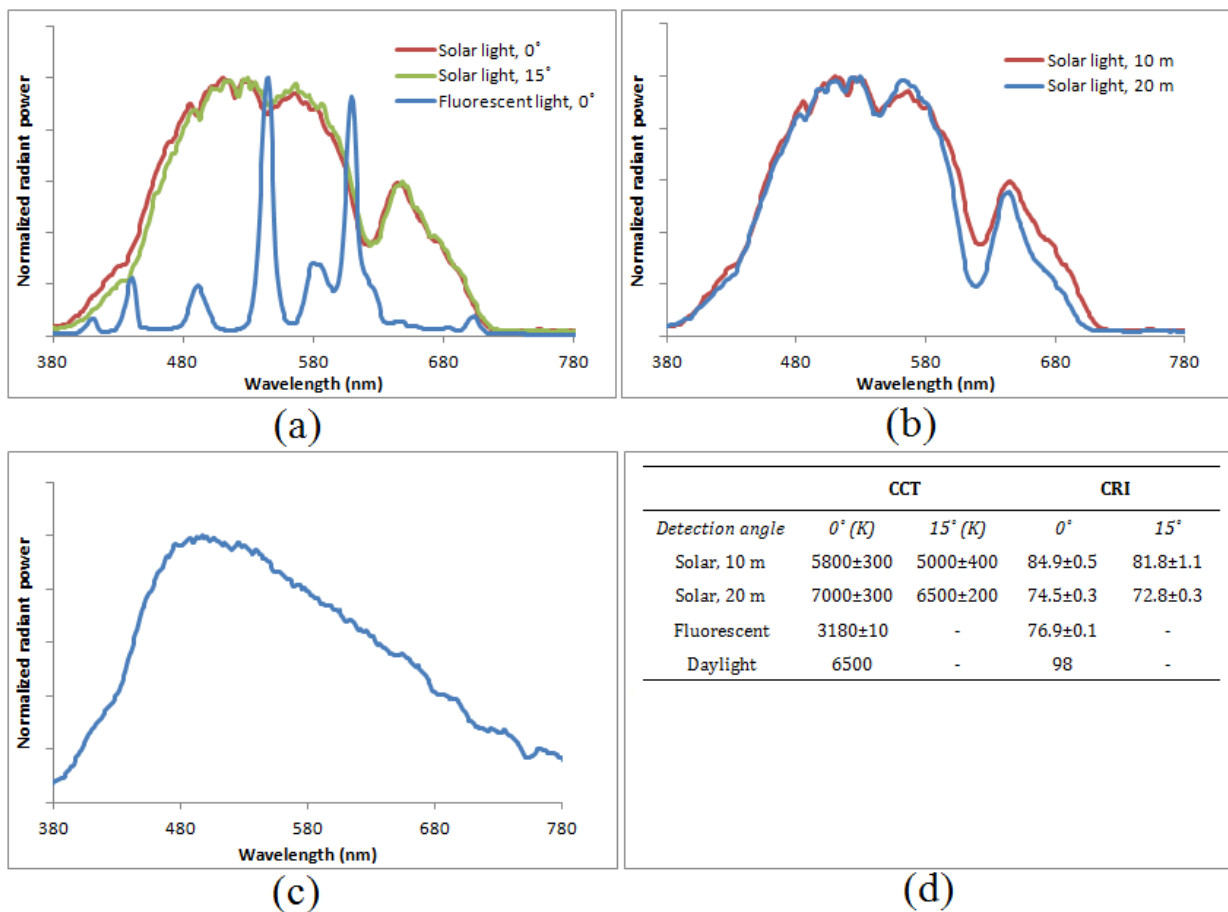


Figure 44. SPD curves of light sources; a) Solar luminaires (10 m) with varied detection and fluorescent luminaire, b) Solar luminaires after 10 m and 20 m optical fiber, respectively, c) daylight spectrum, d) table of the CCT and CRI of the different light sources.

5.2.5 The coupling efficiency

The direct solar luminous flux that strikes the area of the SP3 collector can be compared with the flux leaving the solar luminaires. On a clear day of 130 klx, the luminous flux output of the 10 m POF system was 4600 lm. Given that the total collector area is 0.152 m², the luminous flux on the collector is 19800 lm, which means that the system has a coupling efficiency of 23 %. The coupling efficiency of the 20 m POF system is 15 %.

5.2.6 Results from the survey

The survey was added late in the work, and the number of respondents (33) was too small for a meaningful statistical analysis. Figure 45 shows the result of the survey when categorizing the respondents into three groups when the light source was; (1) solar light (10 resp.), (2) alternating solar and artificial (8 resp.) and (3) artificial, (15 resp.). Every question (Q1-Q17) gave a point (1-7) on a seven grade scale where a 7 not always is the most positive answer (see the questionnaire in Appendix A). The bars represent +/- a standard deviation. Since the number of respondents was too small, qualified conclusions of the result are hard to compile. As expected, group 2, thought the light was more varied (Q13) than the other respondents. The artificial light was considered less flickering (Q11). The perceived flickering of the solar luminaires could depend on thin clouds moving quickly between the sun and the SP3 collector. Question Q0 was a control question about how often the students visited the study area and was not used for the categorization of the respondents. Overall the study show no significant discrepancy between the artificial and solar light sources.

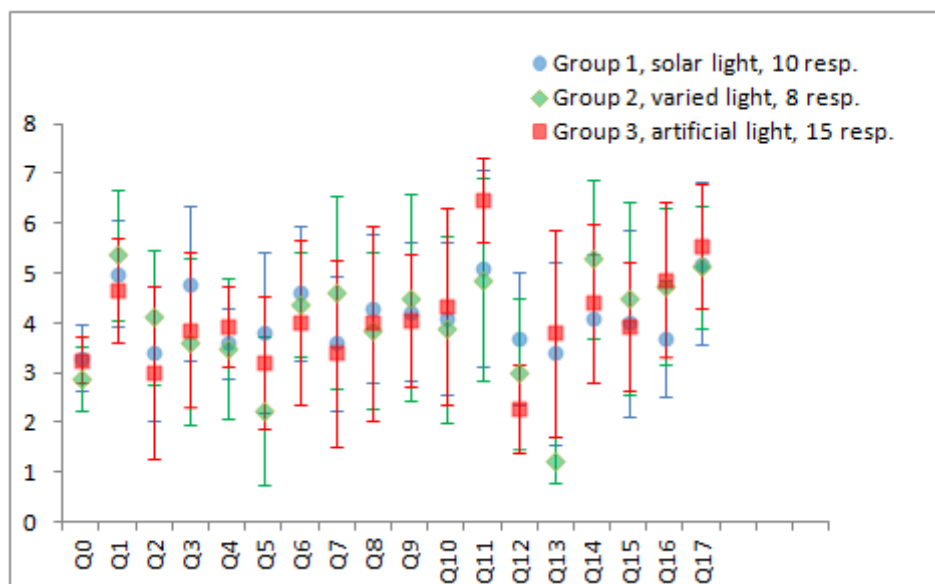


Figure 45. The answers from the survey about the lighting environment at the test site.

5.3 Balancing of the artificial light

5.3.1 Control signal from pyranometer

Like predicted the correlation between the luminous flux output at the test site and the global horizontal irradiance was poor ($R^2=0.57$) as Figure 46a) illustrates.

According to Figure 35, three different configurations of the Kipp & Zonen pyranometer were tested for balancing the illumination at the test site. The first, without any black tube was proven to work ($R^2=0.89$, figure 45b). Secondly the tube and filter were installed to mimic the numerical aperture of the fibers. The correlation seemed good at the beginning, but after 2 weeks the calibration of the signal of the pyranometer had drifted, giving a signal about 10 000 lx below a manually measured direct sun illuminance. Water vapor had condensed on the inside of the filter leaving a coating of dirt when evaporated. As can be seen in Figure 47 the transmittance of blue light was lower after 2 weeks of use.

The filter was removed, and during a partly cloudy day, the luminous flux of one solar luminaire was logged and simultaneously the signal from the Kipp & Zonen. The correlation was good ($R^2=0.91$, Figure 46c), a little bit better than without the tube and filter.

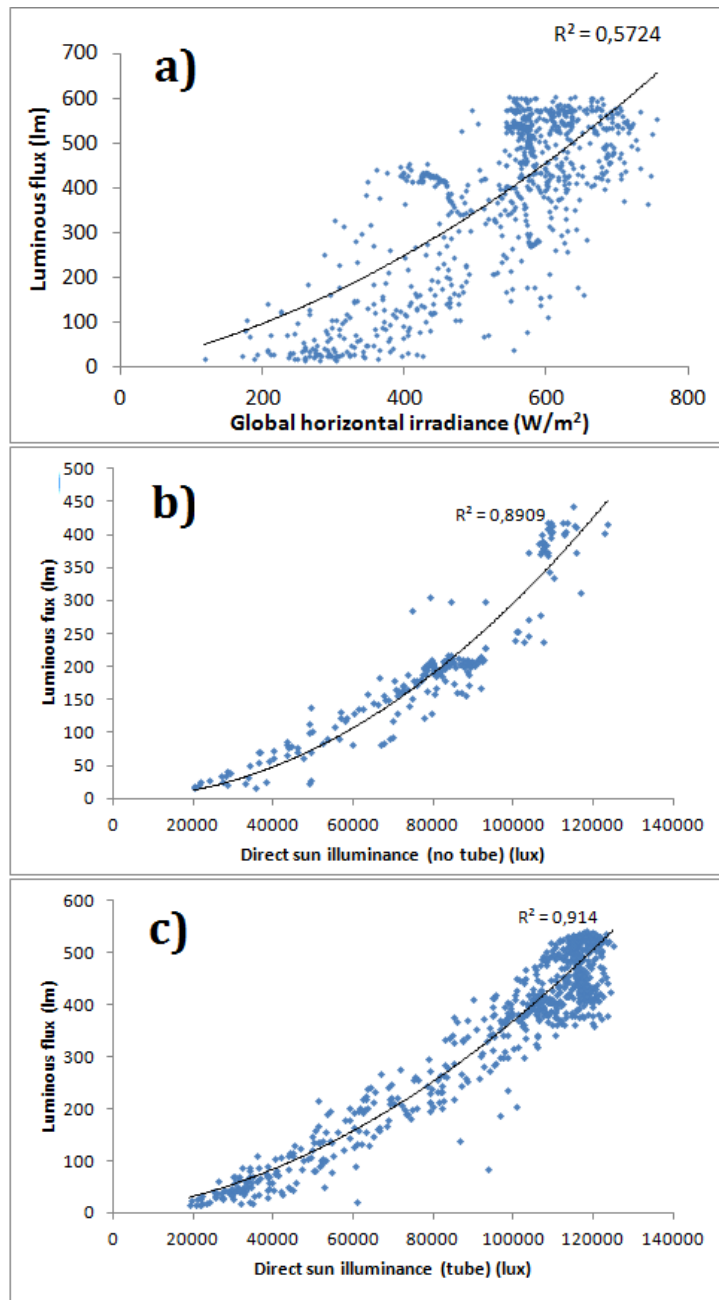


Figure 46. The luminous flux as a function of the a) global horizontal irradiance (W/m²), b) direct sun illuminance (no tube) (lx), c) direct sun illuminance (with tube) (lx).

The measurement series of Figure 46 was done at different occasions and of different length of time series. To avoid strong weighting on the regression analysis of the data logged during cloudy weather conditions, all luminous fluxes <15 lm was removed.

5.3.2 Control signal from indoor illuminance sensors

The tests of the indoor sensors for balancing the artificial lights at the test site were one of the main objectives in this work. A PID regulator was designed using The Ziegler-Nichols tuning method³⁸ for the designing of the PID regulator using the signal from the luxmeter next to the solar luminaire as setpoint. Unfortunately this was done last in the study and therefore no charts illustrating the performance of the regulation system has been made. The regulator seems to work according to comments from the students working in the study hall but variations at partly cloudy days could be annoying, when performing reading tasks. When using the computer or having a conversation the variations were not considered disturbing according to the students. The variations cannot entirely be avoided due to fast weather switches but the response time of the web logging system seemed long and would probably be shorter with a direct control signal from either an outdoor or an indoor sensor.

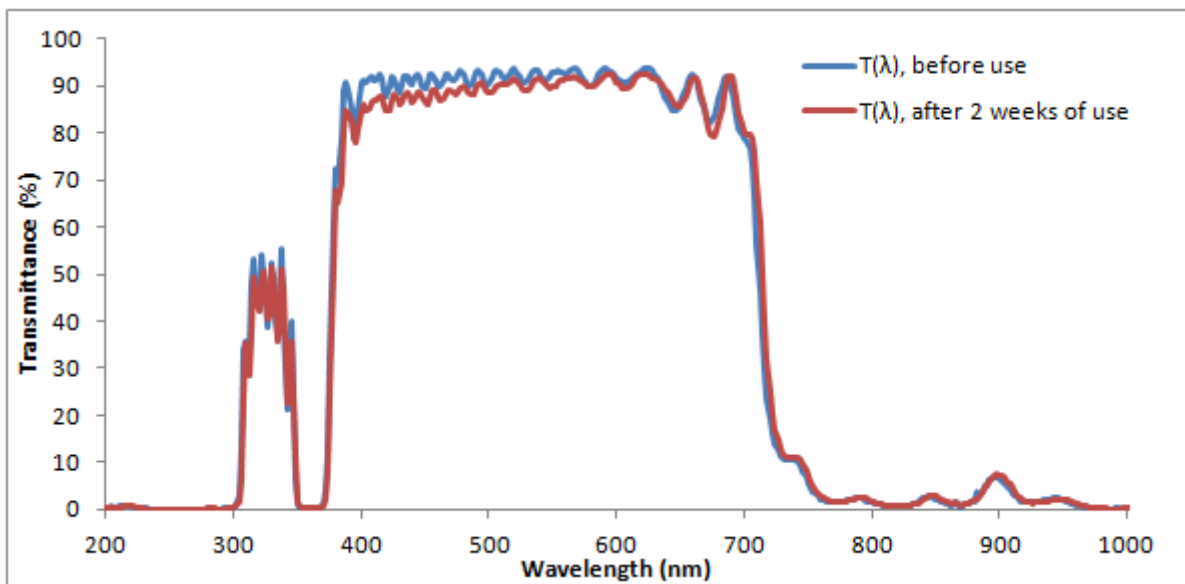


Figure 47. The transmittance of the “TS Hot Mirror NT64-460” from Edmund Optics Inc. before and after 2 weeks of use.

5.4 Energy saving

Due to the limited logging time of the data, the annual power consumption of the system and the dimmable artificial lights had to be estimated. The following assumptions and calculations have been used for the estimation.

The annual power consumption before installing the SP3 system (P_1) and after the installation (P_2) was calculated as;

$$P_1 = P_m * t_{sh} \quad (12)$$

$$P_2 = \underbrace{P_a * t_a + P_p * (8766 h - t_a)}_{\text{SP3 system}} + \underbrace{P_d * t_s + P_m * (t_{sh} - t_s)}_{\text{Artificial lights}} \quad (13)$$

where P_m and P_d is defined in Table 4, P_a is the power consumed by the SP3 collector when active and P_p when passive. The times t_{sh} , t_a , t_s are explained below.

Table 4. Power consumption when the artificial lights are max output or fully dimmed.

Ballast	Measured Power (W)	Specified Power (W)
P_d (Dimmed)	60	8
P_m (Max Output)	246	257

In a study hall area like the test site, the artificial lights are turned on at 07:00-20:00 o'clock on holiday-free weekdays, which is approximately 250 days/year. This time is denoted as "study hours". Energy savings are only possible during study hours. The sunrise and sunset varies over the year. Figure 48 shows the sunrise and sunset in Uppsala 2012. The yellow area number represents the total of hours (3954 h) between 07:00 and 20:00 that has daylight. The pink area represents the total daylight hours of the year (4506 h). A normal year there are 1790 hours of sunshine in Uppsala³⁶. Considering a year in average has 365.25 days, the sunshine time of the study hours was calculated as;

$$t_s = \frac{250}{365.25} * \frac{3954}{4506} * 1790 h = 1075 h \quad (14)$$

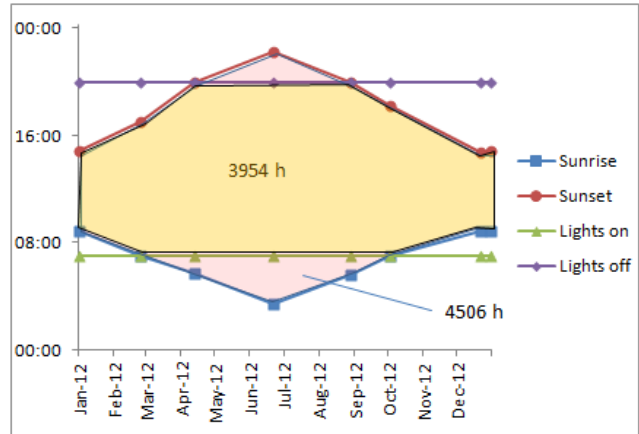


Figure 48. The sunrise and sunset in Uppsala 2012. The yellow area (3954 h) represents the daylight hours between 07:00 and 20:00. The pink area represents the total daylight hours of the year (4506 h).

The sunlight system starts to track the sun 30 minutes before sunrise and stops 40 minutes after sunset. The time of which the Sp3 collector is active was calculated as;

$$t_a = 3954 \text{ h} + 1.1666 \frac{\text{h}}{\text{day}} * 365.25 \text{ day} = 4380 \text{ h} \quad (15)$$

The time of which the artificial lights were on before installing the solar lighting system is the total annual study hours (t_{sh}) and was calculated as;

$$t_{sh} = 250 \frac{\text{day}}{\text{year}} * (20 - 7) \frac{\text{h}}{\text{day}} = 3250 \frac{\text{h}}{\text{year}} \quad (16)$$

The active power (P_a) is higher for our system than specified by Parans because of the old circuit board installed in our system. According to the SP3 specification from Parans, the power consumption is normally 10 W at active time (t_a) and 1.8 W at passive time. But the power consumption varied dramatically between different sites, which depended on a new circuit board installed in some systems. In the specification from Parans the power consumption is 0-10 W. The power consumption of the SP3 system was measured using an energy logger (Voltcraft Energy Logger 4000) to an average of $P_a = 29 \text{ W}$ during the active time.

When fully dimmed the ballast of the artificial luminaires are specified to 3 % (out of 257 W) which means a power consumption of 8 W (Table 4). This does not correspond to the measured power consumption (60 W) though. One explanation could be that the ballast specification of 3-100 % does not correspond to the power consumption but only to the luminous flux of the light resulting in a decrease of the luminous efficacy of the luminaire at a lower luminous flux output.

To illustrate the benefit of installing the system in a location of more sun hours than Uppsala, the potential energy saving if the test site was located in Italy was estimated. Italy has about 3400 sun hours, almost twice the sun hours of Uppsala (1790 h). In Table 5 the energy consumption before installing the solar light system is calculated and after the installation of the system for the system installed in Uppsala and if installed in an area with sun conditions like Italy.

Table 5. The estimated annual power consumption of the test site before and after the installation of the SP3 system. The active power P_a is the measured power using two versions of circuit boards. The power consumption of the test site if situated in Italy is also presented. In parenthesis is the percentage energy saving compared to before the installation of the solar light system.

Circuit board (P_a / P_p)	New (10 W / 1.8 W)		Old (29 W / 1.8 W)	
	Consumption (kWh/year)	Saving (%)	Consumption (kWh/year)	Saving (%)
Artificial lights only (kWh/year)	800	(-)	800	(-)
SP3 and artificial lights, Uppsala (kWh/year)	651	(19 %)	734	(8.3 %)
SP3 and artificial lights, Italy (kWh/year)	429	(46 %)	520	(35 %)

Predictions of higher heat dissipation from the artificial luminaires compared to the solar luminaires were confirmed when comparing logged temperatures next to the luminaires and the wall. The temperatures during a partly cloudy day (19th of September 07.00-20.30) are presented in Figure 49. The load on the artificial lights are represented by the dimmer, where 0 V means fully dimmed and 10 v means max output. These results confirm the thesis that fluorescent lights produce heat, but solar luminaires do not. This graph indicates a potential energy saving, due to decreased need of cooling, but the saving is hard to quantify, because the air flows were hard to control in the test site, where doors are opened and closed throughout the day. If the solar lighting system is installed in a controllable test environment, where the air flow and temperature can be measured, the potential energy saving due to decreased need for cooling can probably be verified.

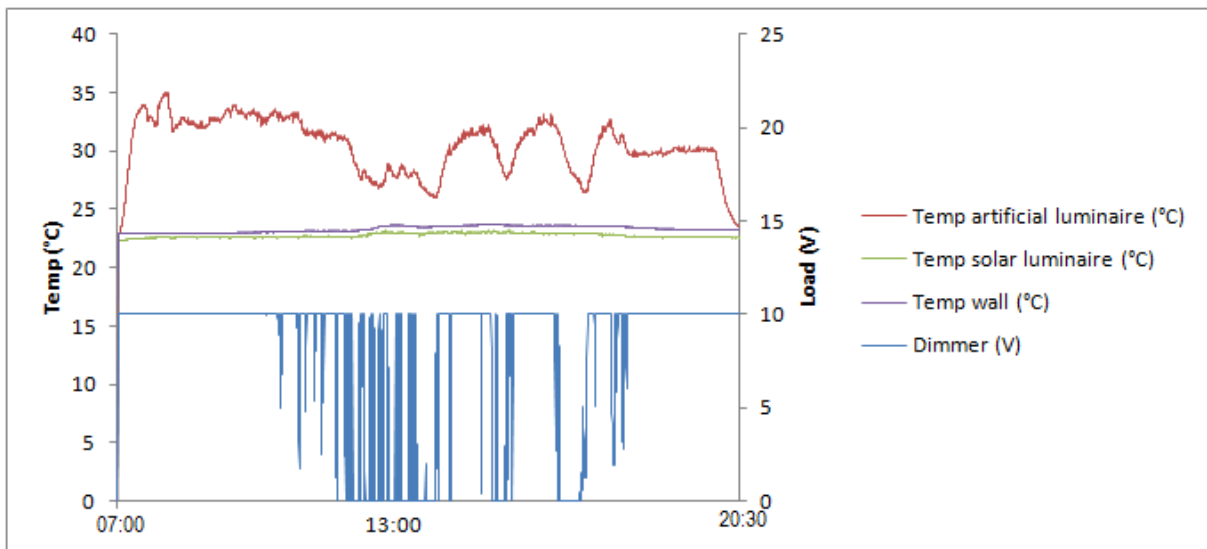


Figure 49. The temperature logged at three different points in the test site; next to the solar luminaire, next to the artificial luminaire and by the wall.

6 Discussion

6.1 Sources of error

- The Kipp & Zonen SP Lite 2 pyranometer used for the direct sun irradiance has a non-linearity of < 1 % at 0 - 1000 W/m² (~ 0 - 100 klx direct sun illuminance). Its temperature dependency is 0.15 %/°C, hence the signal can vary by up to 6 % for the moderate annual temperature variation in Uppsala of -15 °C to +25 °C.
- The Kipp & Zonen pyranometer has a drift, for which an explanation has not been found. A calibration of the pyranometer can a week later drift a few klx at high values of the measurement range (100-130 klx). It is possible that birds have rested on the tube, moving it out of its initial position.
- The response time of the sensors and web logger delays the dimming of the artificial lights at the test site. The Kipp & Zonen has a response time of << 1 s but the response time of the web logger is longer (~2-3 s), visually observed for the light behavior.
- The linearity of the luminous flux measurements is not fully known at high light intensities. The OMIS was calibrated at SP, but only at very low intensities of 2-3 lm (compare; > 800 lm for the best solar luminaires).
- The SPD curves are calculated due to the CIE 13.3-1995 standard, which uses the 2° standard observer (CIE 1931) to adapt the spectrum to the sensitivity of the human eye. However, a recent study shows that the sensitivity of the eye in the blue part of the visual spectrum is underestimated in the standard observer from 1931. A better adapted standard observer developed by Stockman A. 2012 and presented at the “CIE 2012 Lighting Quality and Energy Efficiency” conference is reviewed presently by CIE³⁹.

6.2 Health benefits - Circadian rhythm affected by the spectrum of light

The potential health benefits due to a solar light system are discussed in the introduction. In this section this is exemplified through comments on previous studies on lights impact on the melatonin production, a hormone which controls the sleep/wake cycle. In previous studies the suppression of melatonin production, which means we stay alert, has been shown to be efficient when exposed to blue light of ~440-480 nm and peaking at 460 nm^{7,40,41,42}. One example is a study by Gooley et al⁷ where subjects were spending one night in total darkness and the following night exposed to monochromatic light 460 nm or 555 nm, the latter of which the human eye is most sensitive to. The light session lasted for 6.5 h. Their result showed that the suppression of melatonin is efficient a short period after starting the exposure, when exposed to green light, but the melatonin level in the blood is stabilized back to the same level as the (dark) night before after some time. The melatonin level in the blood for those exposed to the blue light was low during the whole session (Figure 50). The authors suggest that

the cone photoreceptor (visual, sensitive to green) contributes to the melatonin suppression at the start of light exposure and also for low intensities, but the melanopsin photoreceptor (non-visual, sensitive to blue light) contributes at long exposures and high intensities.

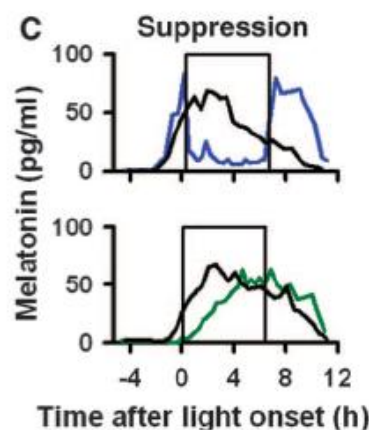


Figure 50. The melatonin level in the blood of subjects exposed to blue (460 nm) or green (555 nm) light. The black curve is the melatonin level the night before. The square represents the time of exposure (6.5 h).⁷

A conclusion that can be drawn from this study is that turning on the fluorescent light in the morning will wake you up, but staying in bed too long will make you drowsy again. To stay alert at work or in school you should be exposed to light of high content of 460 nm light, like daylight. As can be seen in Figure 44a) the content of light around 440-480 nm is much higher in solar light than in fluorescent light sources.

The energy saving of the SP3 system is significant (19 % for Uppsala) but financially the annual saving is modest if considering a price on electrical power of 0.1 €/kWh it is 15 €/year. The economical values of potentially higher production and lower absenteeism at work or school were not studied here, but could be significant according to previous studies mentioned in the introduction and above.

6.3 Lessons learned along the way

When starting this work my understanding of optics and especially fiber optics was limited. Therefore it was hard to estimate the running time of different tasks that needed to be done. Many questions of different nature were sought to be answered and the time needed to satisfactory answer them was hard to predict. For instance the color calculations demanded more time than I could imagine but gave depth to the study. When starting a new project on a subject of which the personnel knowledge is small, the importance of the pre-study naturally increases.

6.4 Future challenges

In today's SP3 system the light from the solar luminaires illuminates a small area with relative high intensity compared to the conventional artificial lights in use at the test site. By spreading out the light over a larger area the solar luminaires can be separated more from each other and the light from the system would be used more efficiently. New diffusers designed for this particular system are being developed in parallel to this study at the same department of Uppsala University.

The system is designed to search the sky for the sun when the power is plugged in, for the convenience of the user. For a climate like Uppsala, with many partly cloudy days, this technique has shown not to be efficient. The risk is imminent that a cloud will cover the sun just as the SP3 collector is about to find the correct position. My suggestion is that the position of the collector should be set up manually by plugging it into a computer (via USB), and then through an interface the collector can be tilted and rotated by the user to the correct position. This is possible today, but a user-friendly interface and easy computer connection possibility is missing.

A reliable control signal for the dimming of the artificial light should be available from the solar light system as a standard accessory, because the supplemented artificial lights are always needed for cloudy and dark times. The signal of the light sensor on the SP3 collector could be used as control signal for balancing the artificial lights. It can be regarded most cost efficient since the sun tracking is fundamental for the system to work and therefore the light sensor is needed independent of the regulation of the artificial lights. The results of these studies show that a tube for limiting the view of the light sensor is not necessary as the accuracy improvement of the control signal is modest (Figure 46). The filter on top of the tube was shown to even worsening the reliability of the signal from the pyranometer, since a vapor coating was built up on the inside of the filter.

An indoor sensor has also been proven an alternative, but then the customer should not have to look for a proper indoor sensor, it should be provided along with the system, and the user should easily be able to set the desired illuminance level in the room. Whether it is trivial or not to design a standard indoor light sensor for different types of interiors needs to be further investigated by the manufacturer of the solar light system and its collaborators.

7 Conclusions

The SP3 system of Parans provide high quality solar light. It has a fuller spectrum compared to the fluorescent lights at the test site, since the spectrum is almost similar to that of the sun despite a couple of absorption dips around 545 nm, 625 nm and 730 nm. These dips affect the color rendering index of the light, which was about 85 (75) through the 10 (20) m fiber system. The light output of the system is somewhat lower than specified by Parans (~500 lm contra 550 lm) for the 10 m system, but slightly higher for the 20 m system (~400 lm contra 350 lm) when the direct sun illuminance was 100 klx. The spatial light distribution of the solar luminaires is limited and wider spreading of the light is desirable.

Saved energy because of decreased need for artificial light is modest in the Swedish climate (19 %, Uppsala) but is significant in southern Europe for instance (46 %, Italy). The solar lights dissipate almost no heat, since the non-visual parts of the solar light is reflected by the filter in front of the input end of the fiber. This could lead to a decreased need of cooling buildings, but the potential energy saving is not fully known yet and further research is needed. There are also potential improvements of the system, by optimizing the lens and switching to glass fibers. However, better quality components must be weighed against the cost.

The best way of dimming the artificial lights was to use the signal from the pyranometer attached to the SP3 collector. The correlation between the direct sun irradiance measured by the pyranometer and the luminous flux output of a solar luminaire was slightly higher when using the black tube (Figure 35) than when not using it. When regulating the artificial lights by the signal from the indoor illuminance sensors problems with oscillation of the artificial lights occurred. If designing the regulator and placing the sensors properly it should be possible to balance the artificial lights by an indoor sensor. Further investigations on a proper indoor sensor regulation are required, but the interiors where the solar luminaires are used vary. Thus a standard configuration of the indoor sensor regulation is hard to produce. Therefore my recommendation is to use the signal from the light sensor on the SP3 collector for balancing the artificial light and find a way to minimize the response time of the regulation, since the sunlight will not wait.

References

- ¹ Hathaway, W. E., Hargreaves, J.A., Thompson, G.W. & Novitsky, D. (1992), *A study into the effects of light on children of elementary school age – A case of daylight robbery*, Alberta Dept. of Education, Edmonton. Planning and Information Services.
- ² Franta, G. & Anstead, K. (1994). *Daylighting offers great opportunities*, Window & Door Specifier-Design Lab, pp. 40-43.
- ³ Liberman, J. (1991), *Light medicine of the future*, Bear & Company Publishing, New Mexico.
- ⁴ Lewy, A. J., Wehr, T. A., Goodwin, F. K., Newsome, D. A. & Markey, S. P. (1980), *Light suppresses melatonin secretion I humans*, *Science*, **210**, pp. 1267-1269.
- ⁵ Philpott, W. H. (1991), *The role of melatonin in the circadian rhythm in health and disease*, *Journal of Orthomolecular Medicine* **6** (3 & 4), pp. 187-190.
- ⁶ Fentemot, J. M. & Levine, S. A. (1990). *Melatonin Deficiency, Its Role in Oncogenesis and Age-related Pathology*, *Journal of Orthomolecular Medicine* **5** (1), pp. 22-24.
- ⁷ Gooley, J. J., Rajaratnam, S. M. W., Brainard, G. C., Kronauer, R. E., Czeisler, C. A. & Lockley, S. W. (2010), *Spectral Responses of the Human Circadian System Depend on the Irradiance and Duration of Exposure to Light*, *Science Translational Medicine*, **2** (31), pp. 31-33.
- ⁸ Edwards, L. & Torcellini, P. (2002), *A literature review of the effects of natural light on building occupants*, National Renewable Energy Laboratory, Colorado, USA, NREL/TP-550-30769.
- ⁹ Romm, J. J. & Browning, D. W. (1994), *Greening the building and the bottom line: Increasing productivity through energy-efficient design*, Rocky mountain Institute, Colorado, USA.
- ¹⁰ Nicklas, M. G. & Bailey, G. B. (1997), *Daylighting in schools*, *Strategic Planning for Energy and the Environment*, **17** (2), pp. 41-61.
- ¹¹ Thayer, B. M. (1995), *Daylighting and productivity at Lockheed*, *Solar today*, **9** (3), May/June, pp. 26-29.
- ¹² Kapany, N. S. (1958), *Colored glass fibers for photographing color TV, or a flexible gastroscope for seeing around the 'corners' of your stomach re possible with... Fiber optics*, The Frontier, publ. Armour Research Foundation of Illinois Institute of Technology, Spring 1958, pp. 18-23.
- ¹³ ASTM Standard G173 (2003), *Standard Tables for Reference Solar Spectral Irradiances: Direct Normal and Hemispherical on 37° Tilted Surface*, ASTM International, West Conshohocken, PA, DOI: 10.1520/G0173-03R08.
- ¹⁴ Committee on Colorimetry of the Optical Society of America (1973), *The Science of Color*, Optical Society of America, 2100 Pennsylvania Avenue, N. W. Washington, D.C. 20037.
- ¹⁵ Schubert, E. F. (2006), *Light emitting diodes, 2nd edition*, Cambridge University press, pp. 275-291.
- ¹⁶ CIE (1987) *The Measurement of Absolute Luminous Intensity Distributions*, Technical report 70-1987. Photocopy 2008, Vienna, Austria.

-
- ¹⁷ CEN (2002), *EN 12464-1:2011*, European Committee for Standardization (CEN), Brussels, Belgium.
- ¹⁸ McCamy, C. S. (1992). *Correlated color temperature as an explicit function of chromaticity coordinates*, *Color Research & Application* **17** (2) pp. 142–144.
- ¹⁹ CIE (1995), *Method of measuring and specifying colour rendering properties of light sources*, Technical report, 13.3-1995, Austria.
- ²⁰ Whitehead, L. A. & Mossman, M. A. (2010) *A Monte Carlo Method for Assessing Color Rendering Quality With Possible Application to Color Rendering Standards*, Wiley Periodicals, Inc. *Color Research & Application*, **37**, pp. 13-22, DOI 10.1002/col.20649.
- ²¹ Davis, W. & Ohno, Y. (2010), *Color Quality Scale*, *Optical Engineering*, **49** (3), art. no. 033602. doi: 10.1117/1.3360335
- ²² Moroney N., Fairchild, M. D., Hunt, R. W. G., Li, C., Luo, M. R. & Newman, T. (2002), *The CIECAM02 Color appearance model*, Final Program and Proceedings - IS and T/SID Color Imaging Conference , pp. 23-27
- ²³ Quintero, J.M., Sudrià, A., Hunt, C.E., & Carreras, J. (2012) *Color rendering map: a graphical metric for assessment of illumination*, *Optics Express*, **20** (5), pp. 4939-4956.
- ²⁴ Hecht, E. (2002), *Optics*, 4th edition, Addison-Wesley.
- ²⁵ Hecht, J. (1999), *Understanding Fiber Optics – 3rd edition*, Prentice Hall, Upper Saddle River, New Jersey, Columbus, Ohio.
- ²⁶ Kaino, T. (1987), *Preparation of plastic optical fibers for near IR-region transmission*, *Journal of Polymer Science, Part A: Polymer Chemistry*, **25** (1), pp. 37-46.
- ²⁷ Izawa, T. & Sudo, S. (1987), *Optical Fibers: Materials and Fabrication*, KTK Scientific Publishers & D. Reidel Publishing Company.
- ²⁸ Mitsubishi International Corp. *Influence of UV on attenuation*, URL: http://fiberopticpof.com/pdfs/Plastic_Fiber_Optics_&_Cable/ESKA_Testing_Data/Durability_to_UV_Light.pdf, retrieved 2012-09-04.
- ²⁹ Goos, F. & Hänchen, H. (1946), *Ein neuer und fundamentaler Versuch zur Totalreflexion*, *Annalen der Physik* **6** (1), WILEY-VCH Verlag GmbH & Co.
- ³⁰ Parans solar lighting AB (2011), *SP3 Receiver*, URL: <http://www.parans.com/eng/customerservice/documents/20111220ParansProductspecifications.pdf>, retrieved 2012-08-15
- ³¹ Himawari (2009), *Lens focusing and optical fiber transmission devices: Solar lighting system Himawari*, URL: <http://www.himawari-net.co.jp/e-pdf/New-Himawari-Catalogue-090518-1.pdf>, retrieved 2012-08-09.
- ³² Sunlight Direct LLC (2012), *TR5-1 Technical specifications*, URL: <http://www.sunlight-direct.com/wp-content/uploads/2012/06/TR5-Datasheet-5-8-12b.pdf>, retrieved 2012-08-16

-
- ³³ Jiangxi Daishing POF Co., Ltd (2012), *Cool light on hot days: Fiber optics bring the sun indoors*, URL: <http://www.dspof.com/en/support-pgdetail-153.html>, retrieved 2012-08-16.
- ³⁴ Nostell, P., Roos, A. & Rönnow, D. (1999) *Single-beam integrating sphere spectrophotometer for reflectance and transmittance measurements versus angle of incidence in the solar wavelength range on diffuse and specular samples*, *Review of Scientific Instruments* **70** (5), pp. 2481-2494.
- ³⁵ Küller, R. & Wetterberg, L. (1993), *Melatonin, cortisol, EEG, ECG and subjective comfort in healthy humans: Impact of two fluorescent lamp types at two light intensities*, *Lighting Research Technology*, **25** (2) pp. 71-81.
- ³⁶ Volotinen, T., Nilsson, N., Johansson, D., Widén, J. & Kräuchi, P. (2011), *Solar Fibre Optic Lights – Daylight to Office Desks and Corridors*, *The Proc. Of the CISBAT11 conference*, 14-16 Sept. 2011.
- ³⁷ Mayhoub, M. S. & Carter, D. J. (2012), *Hybrid lighting systems: Performance and design*, *Lighting Research and Technology*, **44**, pp. 261-276.
- ³⁸ Ziegler, J. G & Nichols, N. B. (1942). *Optimum settings for automatic controllers*. *Transactions of the ASME*. **64**. pp. 759–768.
- ³⁹ Stockman, A. (2012), *Physiologically-based colour matching functions*, *Proc. of the “CIE 2012 Lighting Quality and Energy Efficiency” conference*, 19-21 Sept. 2012, IT06, pp. 49-58.
- ⁴⁰ Lockley, S. W., Brainard, G. C. & Czeisler, C. A. (2003) *High Sensitivity of the Human Circadian Melatonin Rhythm to Resetting by Short Wavelength Light*, *J Clin Endocrinol Metab*, **88** (9), pp. 4502-4505.
- ⁴¹ Lockley, S. W., Evans, E. E., Scheer, F. A. J. L., Brainard, G. C., Czeisler, C. A. & Aeschbach, D. (2006), *Short Wavelength sensitivity for the direct effects of light on alertness, vigilance, and the waking electroencephalogram in humans*, *Sleep*, **29** (2), pp. 161-168.
- ⁴² Thapan, K., Arendt, J. & Skene, D. J. (2001), *An action spectrum for melatonin suppression: evidence for a novel non-rod, non-cone photoreceptor system in humans*, *Journal of Physiology*, **535** (1), pp. 261-267.

Appendix A – Questionnaire for evaluation of the lighting environment

Uppsala Universitet, 2012

Hej!

Det här är en enkät angående ljusupplevelsen i det här rummet. Jag går i ES5:an och gör mitt exjobb där jag utvärderar ett solbelysningsssystem. Solljuset koncentreras på taket och leds in genom 10 meter optiska fibrer. Om det är soligt ute så ser du ett starkt sken från 6 små armaturer ovanför dig. Slå dig ner vid bordet under sollamporna och besvara frågorna nedan. Du får gärna svara även om solen har gått i moln. Det tar max 5 minuter.

Tack för hjälpen!

Hur ofta sitter du i denna lokal?

Flera gånger/vecka 1 gång/vecka Någon gång ibland Första gången

Datum: _____ **Klockslag:** _____:

HUR UPPLEVER DU LJUSET I DET HÄR RUMMET?

Markera genom att sätta kryss i nedanstående skalor.

Mörkt	<input type="checkbox"/>	Ljust						
Behagligt	<input type="checkbox"/>	Obehagligt						
Ofärgat	<input type="checkbox"/>	Färgat						
Starkt	<input type="checkbox"/>	Svagt						
Utspritt	<input type="checkbox"/>	Koncentrerat						
Varmt	<input type="checkbox"/>	Kallt						
Ojämnt fördelat	<input type="checkbox"/>	Jämt fördelat						
Hårt	<input type="checkbox"/>	Mjukt						
Diffust	<input type="checkbox"/>	Fokuserat						
Naturligt	<input type="checkbox"/>	Onaturligt						
Flimrande	<input type="checkbox"/>	Flimmerfritt						
Klart	<input type="checkbox"/>	Murrt						
Varierat	<input type="checkbox"/>	Enformigt						
Milt	<input type="checkbox"/>	Skarpt						
Bländande	<input type="checkbox"/>	Avbländat						
Dämpat	<input type="checkbox"/>	Lysande						

HUR BRA TYCKER DU DET GÅR ATT SE I DEN HÄR BELYSNINGEN?

Mycket dåligt Mycket bra

Innan du är färdig, ta en titt på klockan igen!

Klockslag: _____:

Tack än en gång för hjälpen!

Hälsningar David Lingfors, ES5